Universidad Carlos III of Madrid

Department of Electrical Engineering

Ph. D. Thesis

TRANSIENT VOLTAGE DISTRIBUTION ALONG LV MOTOR WINDINGS FED WITH PWM CONVERTERS. INSULATION AGEING ANALYSIS.

Author: Juan Manuel Martínez Tarifa.

Supervision: Javier Sanz Feito and Hortensia Amarís Duarte.

Dissertation at Leganés (Madrid), on November the 24th, 2005

Board Members:
Alonso A., Universidad Politécnica de Madrid.
Baselga J., Universidad Carlos III de Madrid.
Lebey T., CNRS Toulouse.
Usaola J., Universidad Carlos III de Madrid.
Burgos M, Universidad de Sevilla.

Index:

1.- Introduction and Objectives[1].

Induction motor reliability and robustness has favoured its usage in low voltage industrial applications. Despite this, the main disadvantage from these motors is their stiffness in its torque-speed curves that make it difficult to adjust the motor speed. That's the reason to introduce frequency converters in order to control motors speed. In this sense, one of the most used applications is low voltage induction motor fed by scalar- or vector-controlled Pulse Width Modulation (PWM) inverters.

As it is shown in this work, this type of supply has led to premature failures in the machine's insulation systems, and thus, economic losses due to outages in production. All authors consider that these waveshapes are responsible for these unexpected failures within the stator windings, whose insulation systems were designed for power frequency supplies.

In this work there will be, first of all, a *bibliographical review* about the most important elements that influence motor's lifetime. In this sense we will show a review about models and measurements referred to voltage distribution along windings subjected to transient pulses, and the inverter-motor cable effect will be mentioned as well. Finally, the main motor and insulation systems diagnosis techniques already existing will be reviewed.

Published works make sure that turn by turn voltage distribution prediction along random wound coils is an important problem in order to quantify motor's stresses and still remains to be solved. A first approach facing this problem, is to propose a winding theoretical model and analyse possible assumptions. The *third chapter* will allow to face this task through a theoretical model for voltage calculus in the frequency domain applied to a five-turn random wound coil. In order to model some complex electromagnetic phenomena from the point of view of a distributed parameter equivalent circuit some assumptions must be made. Afterwards, all the parameters from the equivalent circuit defining the unit cell, will be characterized in the frequency domain. Model calculation will be compared to experimental measurements. Model reliability to calculate turn by turn voltages in different random wound coils was also studied. The accuracy of this methodology was analysed too when some of its parameters or effects were neglected. Finally, in order to apply this model to voltage calculation in real random wound coils, voltage propagation measurements along a real motor stator winding were made.

This previous work helped to face the model application to coils with higher number of turns, and, simultaneously, make the necessary simplifications in order to avoid complex sides from the system without interest. This was made in *chapter four*, where computed voltages in the high frequency range were compared to experimental measurements. The

[1] This report is a review from the original Ph.D. document published in Spanish. Most figures hold the names and labels from this original document. For more information, please contact to the author by e-mail (jmmtarif@ing.uc3m.es)

same parameters than in the previous chapter were neglected in order to study the effect of theses simplifications into voltage calculation. As frequency domain calculation were successful, inverse fast fourier transform (iFFT) was applied to these data to calculate time domain voltages. Finally, the model was applied to calculate voltage propagation of transient pulses with values of *du/dt* as those found in many industrial environments.

Chapter five was devoted to the application of frequency response analysis (FRA) techniques to evaluate turn-to-turn insulation status, and to find new coil designs that may allow to minimize turn-to-turn electrical stresses. In order to achieve this, the high frequency voltage calculation model was applied to varnished coils and stray capacitances were pointed as main factor in voltage distribution of applied pulses. The last section from this chapter was devoted to study FRA applications into turn-to-turn dielectric status after partial discharge (PD) ageing.

2.- Insulation systems in induction motors fed with PWM inverters.

2.1.- Introduction: Causes and Consequences for insulation damage.

2.1.1.- Uneven voltage distribution through the windings.

When PWM inverters feed induction motors, it must be kept in mind that steep fronted pulses with rise times of about 200ns, have high frequency spectral components. In this case, stray capacitances due to different insulation systems (turn to turn and turn to ground) become more important in turn by turn voltage propagation ([Narang, 1989], [Kaufhold, 1996], [Stone, 2000]). This high frequency behaviour explains that voltage distribution along each phase stator winding has an irregular pattern ([Kaufhold, 1996], [Melfi, 1998], [Bidan, 2001], [Popov, 2003]). Moreover, nearly the whole input transient voltage is developed in the first coil of the winding ([Manz, 1997], [Toliyat, 1999], [Oyegoke, 2000], [Bidan 2003], [IEC 60034-17]). That is why it would be very interesting to achieve previous voltage distribution calculation in order to reinforce certain insulation systems.

2.1.2.- Overvoltages applied to the machine.

In industrial applications, the most common configuration is placing inverter and motor at different locations and connecting them by a power cable of some tens or even hundreds of meter long. In these cases, impedance mismatch between cable and motor may be suitable for electromagnetic waves reflection phenomena ([Greenwood, 1991]). As can be seen from the example presented at Figure 2.1, this will provide up to 2p.u. transient overvoltages at the machine's input terminals ([Manz, 1997], [Bonnett, 1998], [Lee, 2004], [Hanigovszki, 2004]).

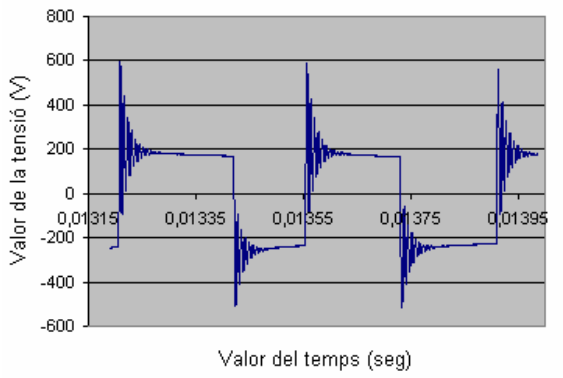

Figure 2.1.- Terminal overvoltages at one 1.5kW ASD with 300m cable length..

It has been reported that overvoltage magnitude depends on power rating, rise time and cable length ([Von Jouanne, 1996], [Lee, 2004]). Other works point to the possibility that up to 4p.u. overvoltages may occur due to polarity reversal and double pulsation ([Kerkman, 1997], [Hanigovszki, 2004]).

2.1.3.- Consequences from the application of these new electrical stresses.

As low voltage induction motor windings have a random nature, it is fairly possible that any physical contact between the first and last turns in the coils may appear ([Suresh, 1997], [Stone, 2000]). Machine's overvoltages in addition to uneven voltage distribution through the coil enhance electrical stresses on turn to turn insulating systems so it becomes the electrically weaker point of the winding ([Mbaye, 1997], [Islam, 1997], [Fabiani, 2001], [Bidan, 2003]). In fact, turn-to-turn insulation breakdown has been identified as a main cause of failure even in form wound coils ([Mclaren, 1988], [Wen, 2004]). One immediate consequence arising from these stresses is the presence of voltages spikes above the DIV, so PD's are responsible for turn-to-turn insulation ageing and may lead to its breakdown ([Melfi, 1998]). Once turn insulation has been punctured, this allows a very high current to flow in the affected copper turn leading to burning/melting the groundwall insulation ([Melfi, 1998]).

2.1.4.- Current research activities.

In order to understand these problems, main research activities have been devoted to the following fields:

1) Voltage distribution analysis along motor windings.
2) Overvoltage prediction.
3) Search for ageing indicators related to remaining lifetime from motors insulating materials.

In this chapter it has been summarized models and methodologies used in the read bibliography.

2.2.- Methodology for transient voltages distribution analysis in electrical machines subjected to impulses.

2.2.1.- Classical model calculation applied to transformers.

Classical models have been applied to transformers when they are subjected to lightning and switching impulses ([Wagner, 1915], [Karsai, 1987]). Their analytical solution allows calculating voltage distribution along the windings, but they have some disadvantages: These models neglect losses and mutual indutances, they do not provide any experimental comparison, and the analysis is not valid for inverter-fed steep fronted pulses and random wound coils ([Wagner, 1915]).

2.2.2.- Former models based upon multiconductor transmission line theory.

Former models applied to rotating machines used multiconductor transmission line methodology. In the equivalent circuit, stray capacitances were calculated using the parallel plate capacitor approximation. Calculation of inductances was made supposing TEM wave propagation through the windings ($L*C=1/v$). The analytical solution obtained by using convolution theorem or inverse Fourier Transform was compared successfully to experimental voltage distribution through the windings ([Wright, 1983], [McLaren, 1988]). On the counterpart, the analysis was only valid for non-repetitive transients with rise times higher than 100ns, so many authors still neglected losses and mutual inductances ([McLaren , 1988], [Narang, 1989]). In addition to this, the model was only applied to form wound coils.

2.2.3.- Recent methodologies based upon multiconductor transmission line theory.

Lower rise times make mandatory to account for losses in the models for voltage distribution calculation ([Oyegoke, 2000], [Bidan, 2001]), for example. This is also related to electromagnetic high frequency phenomena that should be considered. This is the reason of using Finite Element Method (FEM) to support element calculation in multiconductor transmission line models. When using this method, different meshes were applied to the geometry under calculation in order to calculate electric and magnetic fields within the stator. This has allowed making some discussions about parasitic resistances, self and mutual inductances and stray capacitances at higher frequencies ([Jianru, 2002], [Hwang, 2003], [Lupo, 2002]). However, due to FEM software complexity, parameters calculations were made at a single frequency. Moreover, models were only applied to form wound coils.

2.2.4.- New models based in distributed parameters equivalent circuits.

Recently, it has been developed distributed parameter equivalent circuit models where each single elementary cell corresponds to one turn. The main differences between different approaches are the software tools used for time domain voltage distribution calculation (EMTP, SPICE, Simulink…). As electrical parameters calculation is a complex problem to be solved with approximations in random wound coils, FEM methods are also used ([Toliyat, 1999]). As mentioned before, FEM methods are applied at a single

frequency, while steep fronted pulses have a widespread spectral content; this leads, for example, to skin effect calculation errors. None of these works takes into account proximity effect ([Toliyat, 1999], [Al-Ghubari, 2001]).

2.3.- Insulation ageing indication.

2.3.1.- Resistance measurements.

One of the most used *Off-Line* techniques is the insulation resistance tests. They are applied to machines diagnosis as they are able to detect those affected from pollution and moisture ([Florkowski, 2003]). They are also good for detecting major flaws where the insulation is cracked and thermal deterioration and loose coils in form wound stators using thermoplastic insulation systems ([Stone, 2005]).

The resistance is measured using a high voltage DC source and a nanoammeter. As this parameter shows great temperature dependence, it is used the polarization index too: this is the quotient of the resistance values after 10min and 1min of applied voltage.

Its main disadvantage is that for clean and dry dielectrics, measured resistance values are very high even near to its final breakdown (Kueck, 2002]).

2.3.2.- PD detection.

Up to now, PD detection is the most extended non-destructive test in motor diagnosis. That's why its application into ASD's motors is the most used one. Following [Stone, 2005], pulse magnitude is proportional to void size where the PD took place; this event is more probable in great flaws than in small ones, so PD test may detect winding status in its more aged area.

The only *On-Line* test applied to stator windings *for power frequency* is PD detection. There have been different approaches trying to set ageing indicators regarding to its data:

1) Analysis of PD patterns. PD pulse height distribution analysis has been tried to be related to degradation process evolution in PD sites ([Contin, 1993]).
2) Graphical representation of PD amplitude vs its rate. This may allow to distinguish between the activity due to different PD sites in the winding ([Lyles, 1988]).
3) Discharge pulse sequence analysis has allowed to diagnosis "treeing" and the number of flaws in the insulation ([Patsch, 2002]).

On the counterpart, following Guide IEEE Std 1434-2000, there are clear difficulties when extracting conclusions from PD measurements since acceptable PD activity levels may change from type to type of insulation system. In fact, it has been remarked that PD measurements are not expected to detect any problem that an insulation system may be prone to ([CIGRE, 1998], [IEC 60034-25, 2004]). Despite this is added to

capacitance and tgδ measuring bridges, there is no unique defined test to detect any insulation problem.

On the other hand, LV machines operating at 50Hz were not expected to be subjected to PD, so for motors rated below 2.3kV, PD tests have not ever been applied ([Bartnikas, 1979], [Stone, 2005]). The progresses in power electronics applied to ASDs have overwhelmed these limits.

Regarding to *On-Line PD detection in inverter fed drives*, up to the date, there is no reliable method due to the technical difficulties of discriminating the voltage steep-front itself from the PD event in the frequency domain, because both of them take place in the ns range ([Manz, 1997], [Bidan, 2003]). This is the reason of making PD tests on twisted pairs of enamelled magnet wire ([Mbaye, 1998], [Hayakawa, 2005]). In order to measure motor's DIV, only *off-line* techniques have been developed ([Bidan, 2003],[Fenger, 2003]).

DIV can be detected *on-line* by PD light intensity measured with a photo multiplier tube and a still camera with image intensifier. This has been applied to twisted pairs samples ([Hayakawa, 2005]) and would require a correlation between charge magnitude and light intensity.

2.3.3.- Dielectric spectroscopy and frequency response analysis.

Ageing process has a great influence on the material dielectric properties. Among them, ε is presented as an ageing marker since its changes grow with energy dissipation ([Pouilles, 1995]). That's the reason to measure this parameter in a high temperature and frequency range in order to study the material relaxation processes: this is the *dielectric spectroscopy*.

In the same way, impedance measurements in a high frequency range may be useful to study insulation's physical and chemical properties ([Guilhaume-Chaillot, 2004]). This *Frequency response analysis* (FRA) has been used in mechanical distortion measurement in transformers' and wind energy generators' windings subjected to shortcircuits ([Florkowski, 2003]).

Despite this is an off-line technique, data acquisition is fast, accurate and repetitive; sample preparation is simple and, in addition to its non-destructive character, allows to analyse different polarization mechanisms involved in the ageing process ([Guilhaume-Chaillot, 2004]).

2.3.4.- Other tests.

In order to find big flaws in the winding insulation, a *high potential test (Hipot)* is applied to it where test voltage (AC or DC) is higher than rated one. The idea is that if the winding does not fail as a result of the high test voltage, it is not likely to fail anytime soon after due to insulation ageing when it is returned to service. If a winding fails the test, then a repair or rewind is mandatory, since the groundwall insulation has been punctured

([Stone, 2005]). It is a go/no-go potentially destructive test, so it cannot make an ageing diagnosis.

Polarization and depolarization currents measurements allow making some ageing diagnosis in oil-paper insulation systems. It works applying a high DC voltage to a dielectric sample and measuring the stray current (~pA) through it in the charge (polarization)-discharge (depolarization) processes ([Zaengl, 2003]).

Recovery voltage meter is also applied to power transformers in order to measure the moisture content from its insulation systems. The process starts with a high DC voltage subjected to the specimen during *Tc*, and finishes with a shortcircuit in its terminals during *Td* (*Tc/Td=2*). After *Tc+Td*, the maximum voltage in the dielectric due to the depolarization process is measured ([Zaengl, 2003]).

The surge tests measure turn-to-turn insulation integrity in form wound stators by applying a high voltage impulse between turns. In acceptance tests ([IEEE 522, 2004]), surge must have 100ns rise time and 3.5p.u. amplitude while in maintenance tests, the amplitude is 2.5p.u. Any shortcircuit is measured by an LC resonant circuit. As a Hipot test, it is a potentially destructive one that does not provide any information about ageing status

3.- Calculation model and analysis of turn by turn voltage propagation.

3.1.- Objectives.

Firstly, this chapter was devoted to a previous approximation to the problem of turn by turn voltage calculation in random wound coils. To this purpose, it was proposed a distributed parameter equivalent circuit model where it must be defined all the parameters from each cell. In the same way, it will be proposed some equations in order to model some electromagnetic phenomena (turn to turn mutual inductance, proximity effect…) which imply difficult circuital simulations. Before running the model in a five-turns random wound coil, it was made some measurements of different parameters from each cell in a form wound coil, so it was possible to make a better analysis about the importance of each parameter in the high frequency model. The accuracy of this methodology was checked with high frequency experimental voltage measurements for all turns at different random wound coils. Once this was achieved, the equivalent circuit was applied in order to study the effect that some simplification on its structure may have on model's reliability.

Finally, in a further step to voltage calculation in motors, it was analysed the turn by turn voltage propagation in a real stator winding subjected to transient voltages with rise times similar as those found in PWM inverters. By this way it was possible to detect which points inside the winding undergo greater electrical stresses, and thus, which turns through it are most relevant for voltage calculation with a reliable model.

3.2.- Model general structure.

Due to the high frequencies involved (above 1MHz), the chosen model was a distributed parameter equivalent circuit where each cell includes not only turn series resistance and reactance, but also stray turn-to-turn and turn-to-ground capacitances (see Figure 3.1). All these measurements were done on the basis of a frequency response analysis (FRA) for each electrical element.

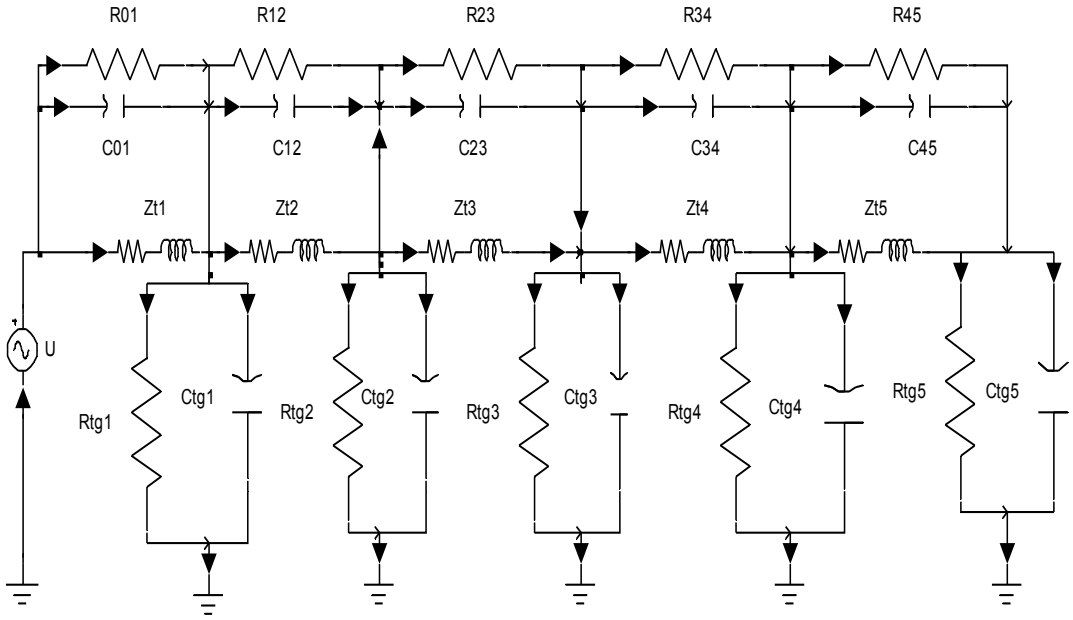

Figure 3.1.- Distributed parameter equivalent circuit model.

One turn series impedance measurement ($Zt(\omega)$) made in a wide broadband allows to take into account series resistance skin effect as well as the frequency dependence of self inductance. Turn-to-turn ($Ztt(\omega)$) and turn-to-ground impedances ($Ztg(\omega)$) have been modelled with an *RC* parallel equivalent circuit that includes, not only their intrinsic dielectric behaviour, but also losses inside them.

3.2.1.- Proximity and skin effects.

Since proximity effect is a complex problem to analyse, it was modelled on the basis of some approximations presented by other authors. After taking into account this effect, series resistance dependence with frequency is set by the following equation:

$$R(\omega) = R_{sk}(\omega) * e^{k} = R_{sk}(\omega) * e^{\sqrt{\frac{f}{f_0}}} = R_{sk}(\omega) * K_{prox}(\omega) \qquad (3.6)$$

where $R_{sk}(\omega)$ is the series resistance which includes skin effect. The criterium followed to make this modelling was assuming as valid the approximation set in [Wright, 1983] for high frequencies, so:

$$K_{prox}(f = f_+) = 6.3333 \qquad (3.8)$$

is a value that is reached just at the highest frequency under analysis (f_+), and has lower values at lower frequencies. This condition allows to calculate f_0 at (3.6).

3.2.2.-Mutual inductances.

Since turn to turn mutual inductances modelling is cumbersome too, it was necessary to assume as valid certain approximations:

$$\mathrm{Zm}_{i,j}(\omega) = j * \omega * M_{i,j}$$
$$\mathrm{M}_{i,j} = \mathrm{k}_m * \sqrt{\mathrm{L}_i * \mathrm{L}_j} \qquad (3.10)$$

where k_m was chosen between 0.7, 0.8, 0.9 and 1 depending on the lower or greater relative proximity between turns in the frontal overhang section respectively ([Gubbala, 1995], [Jianru, 2002]). Self inductances L_i are obtained from series reactance data ($Im(Zt_i(\omega))$) measured previously.

3.2.3.- Other effects.

Temperature can be neglected as a main factor in voltage distribution through the windings ([Neacsu, 2002]), so the application of the model can be made at normal conditions.

Magnetic sheets saturation has a low influence in the study of these transients, because relative permeability is not a main factor compared to stray capacitances through the winding ([Al-Ghubari, 2001]).

3.3.- Model resolution.

On the basis of the presented equivalent circuit, it will be established the equations that arise from the application of the mesh method to this ladder network with five cells (one for each accessible turn) when the coil is fed with a variable frequency sinusoidal voltage source (1V, 0rad). This methodology can be fully understood with Figure 3.3.

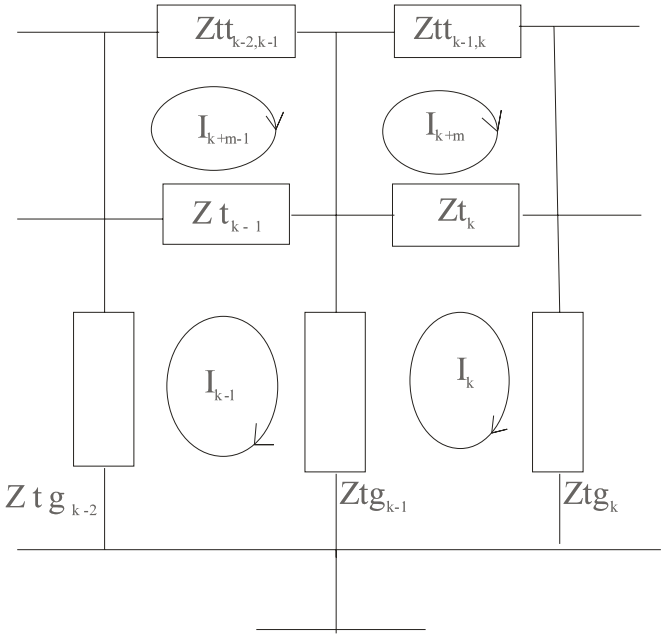

Figure 3.3.- Mesh method application sketch.

Simulation runs of this model for all studied frequencies leads to mesh *i* current calculation I_i, and thus, to the current vector [**I**(ω)]:

$$[\mathbf{U}] = [\mathbf{Z}] * [\mathbf{I}] \Rightarrow [\mathbf{I}] = [\mathbf{Z}]^{-1} * [\mathbf{U}]^t \qquad (3.13)$$

where [**U**(ω)]=[1, 0, 0, 0, 0, 0, 0, 0, 0, 0] is the voltage vector. By using turn-to-ground impedances, wide broadband turn to ground voltages are easily obtained. Solving equations in the frequency domain is the only way of taking into account the previously described electromagnetic phenomena.

3.4.- Experimental acquisition of the model parameters.

3.4.1.- Test cell description.

In this section, it was described the model used as an analogy of an electrical machine stator. In this particular case, turns were wound in a form way in order to analyse how are the different measured impedances depending on the location of the turn in the slot (see Figure 3.5). In addition to this, it was described the characteristics and the connection topology of the impedance analyser used to measure each winding impedance.

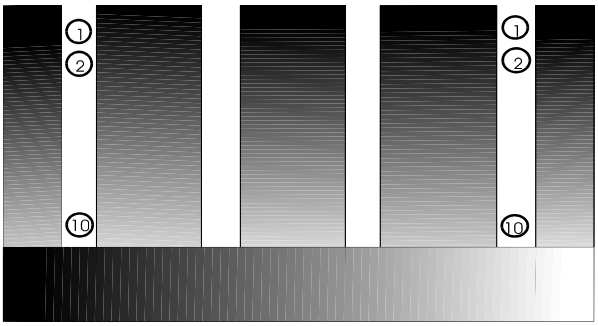

Figure 3.5.- Cross section winding sketch.

3.4.2.- Measurements.

a) Turn Impedance.

The analysis of turn series resistance dependence with frequency shows the appearance of skin effect at high frequencies. In addition to this, different turn lengths lead to different series resistances for each frequency. The analysis of turn reactance inductive character shows that the deeper is the turn into the slot, the bigger is the series reactance due to lower reluctances of the paths associated to stray fluxes.

b) Turn to ground impedance.

Taking into account that dielectrics are modelled as *RC* parallel equivalent circuits, turn to ground series resistance and reactance dependence with frequency, follow the expected behaviour. In addition to this, it must be remarked that turn height in the slot nearly do not have any influence in turn to ground impedance.

c) Turn to turn impedance.

Since turn to turn impedance is another dielectric system, its series resistance and reactance have the same frequency dependence as commented before. In this case, it is shown how electrical coupling between turns is bigger (see Figure 3.13) and series resistance is lower (see Figure 3.14) as turns are closer.

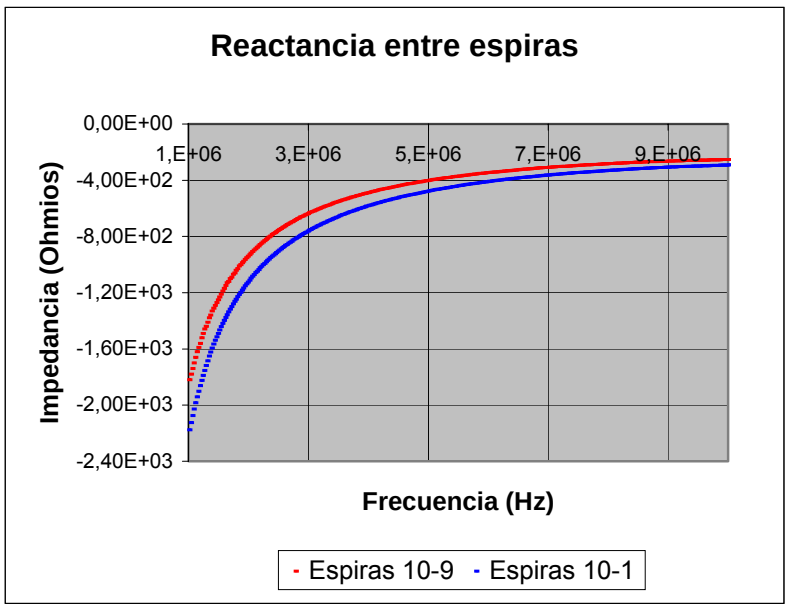

Figure 3.13.- Turn to turn reactance.

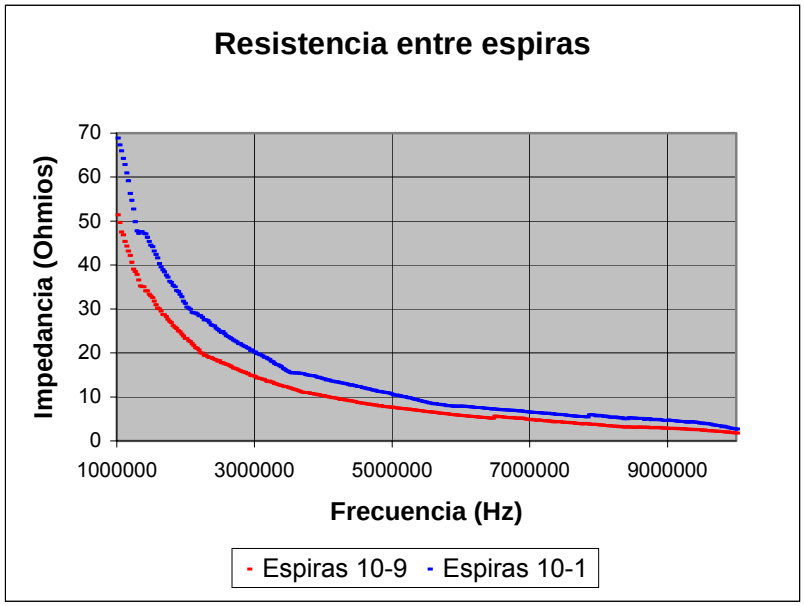

Figure 3.14.- Turn to turn resistance.

3.5.- Preparation and Verification of starting hypothesis from the model.

In order to apply the previously described methodology (section 3.2 and 3.3) it was used the electrical machine stator model from section 3.4.1, and inside it, it was inserted a coil by using five turns from the same manufacturer and with the same length wound in a

random way. Turns may be linked between them by using external connectors without permanent welding.

3.5.1.- Simplifying hypothesis.

Winding modelling was made using the electrical parameters from section 3.4, but, in this case, just one measurement was used to characterize each impedance from the whole winding: turn series impedance, turn-to-ground impedance and turn-to-turn impedance. Random nature of the winding allows justifying this assumption, since, for example, mean turn height in the slot is the same for each turn, mean distance between turns is the same and turn lengths are all the same. These simplifications are resumed in the following equations:

$$\begin{aligned} Zt_i(\omega)&=Zt(\omega) \quad \forall i \in \{1,2,3,4,5\} \\ Ztg_i(\omega)&=Ztg(\omega) \quad \forall i \in \{1,2,3,4,5\} \\ Ztt_{j,i}(\omega)&=Ztt(\omega) \quad \forall i \in \{1,2,3,4,5\}, \ \forall j=i-1 \end{aligned} \tag{3.15}$$

Steep fronted pulses applied to low voltage induction motors provide spectral components up to 5MHz, so we took this value as the maximum one for impedance measurements in winding characterization.

3.5.2.- Analytical solution and comparison with experimental results.

In this section it is shown the results from turn by turn voltage calculation for all frequencies by using the model depicted in section 3.2. Test cell setup allows making some transfer function measurements for all nodes, taking as a reference the same feeding configuration as in the model. As frequency domain interval is the same as the one used for impedance measurements ([100Hz, 5MHz] with 100kHz frequency steps), it is possible the direct comparison between experimental and theoretical frequency dependent voltage distribution (in amplitude and phase) for all turns. The results, as can be seen in Figures 3.16-3.19, show a good agreement between both approaches.

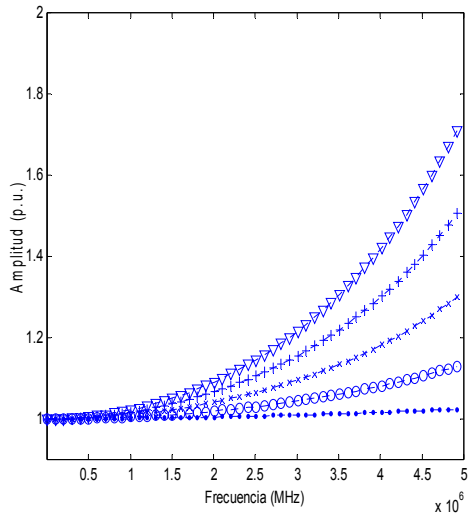

Figure 3.16.- Voltage amplitude at turns #1(●), #2 (❍), #3 (X), #4 (+), and #5 (▽). Results corresponding to the theoretical calculation model.

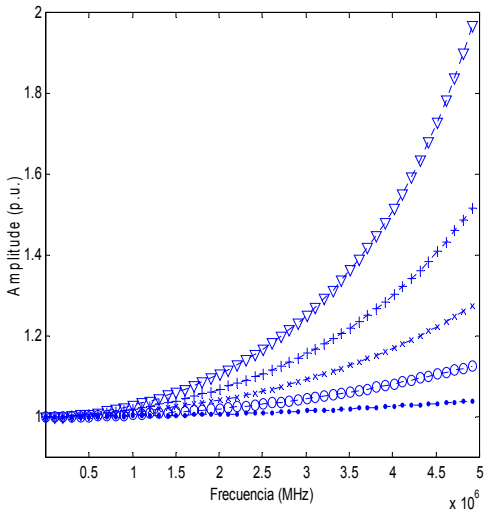

Figure 3.18.- Voltage amplitude at turns #1(●), #2 (❍), #3 (X), #4 (+), and #5 (▽). Experimental results.

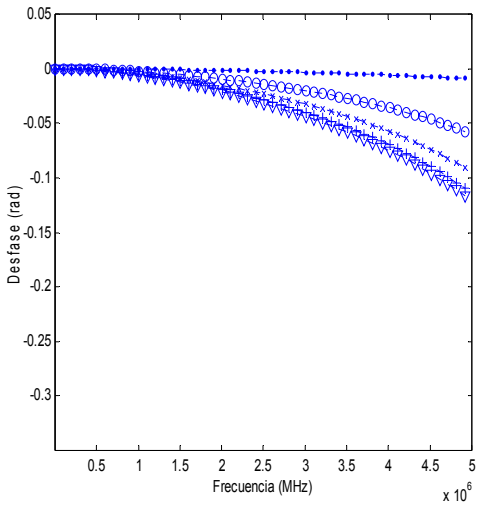

Figure 3.17.- Voltage phase at turns #1(●), #2 (❍), #3 (X), #4 (+), and #5 (▽). Results corresponding to the theoretical calculation model.

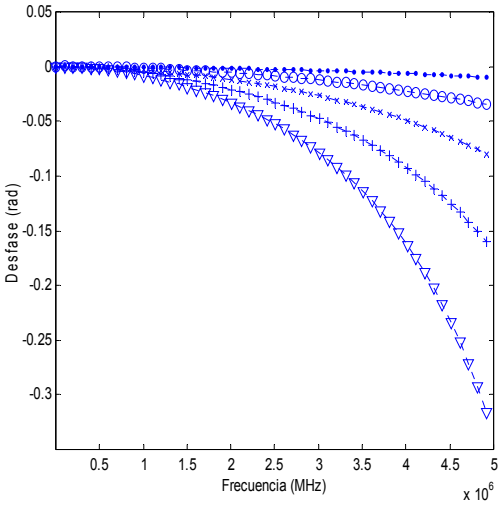

Figure 3.19.- Voltage phase at turns #1(●), #2 (❍), #3 (X), #4 (+), and #5 (▽). Experimental results.

3.5.3.- Model application capability in different samples.

It might be thought that maybe the model would not work properly for different coils, due to their random nature. This is the reason to apply the same methodology to other two five-turns random wound coils, by using just the impedance measurements from another coil (the one from section 3.5.2). In this sense, it is mandatory to define the accumulated absolute errors for all frequencies and averaged for all nodes (both in amplitude and phase) in order to make quantitative comparisons about model reliability. The results presented at Table 3.2 remark that the model makes voltage distribution calculations for all frequencies and nodes independently of the random nature of the coils.

Sample	**Amplitude error (p.u.)**	**Phase error (rad)**
Coil #1	0.0127	0.0133
Coil #2	0.0181	0.0125
Coil #3	0.0157	0.0134

Table 3.2.- Mean accumulated absolute errors (amplitude and phase) for each sample.

3.5.4.- Model sensitivity analysis.

Once model accuracy has been checked, it can be used in order to study the effect that some approximations have on high frequency model calculations. Firstly, neglecting dielectric losses from the model has no effect on calculated errors, so their inclusion is not necessary. In the particular case of neglecting losses due to skin and proximity effect, it was observed greater deviations in voltage phase calculations. On the contrary, voltage amplitude calculations are most affected if mutual inductances were not taken into account in the equivalent circuit. The results are summarized at Table 3.3.

Model	**Amplitude error (p.u.)**	**Phase error (rad)**
Complete	0.0127	0.0133
Neglecting dielectric losses.	0.0127	0.0133
Neglecting losses due to skin and proximity effect.	0.0126	0.0339
Neglecting mutual inductances	0.0770	0.0139
Neglecting either mutual inductances and losses due to skin and proximity effect	0.0763	0.0390

Table 3.3.- Mean accumulated absolute errors (amplitude and phase) for each model.

3.6.- Turn by turn transient voltage propagation analysis in real machine stator windings.

Once a reliable model for voltage calculation is available, the following step would be to apply it into a real coil with a higher number of turns. But, if for a *5* turns coil, it was used a distributed parameter equivalent circuit model with *10* meshes, when applying it into a *n* turns coil, it should be necessary to apply a cumbersome *2n* equations system. This is the reason why, before proceed in this direction, it was studied if it is mandatory to have a prediction model to calculate voltages through all turns in the winding. That is why we treated to measure which points through the first coil in a real machine stator are subjected to greater electrical stresses due to steep fronted transients.

3.6.1.- Experimental setup.

In this section, turn by turn voltage distribution stator coils have been measured in an induction motor subjected to pulses with similar rise times as those presented in real inverters. On this purpose we counted on the material and the experienced skills from the research group in Dielectric Materials applied to Energy Conversion from the Electrical Engineering Department at University Paul Sabatier-CNRS at Toulouse (France). Among the material used, the test object was a low voltage induction motor with 6 coils in each phase with 17 enamelled wires randomly wounded each. The most interesting modification in this standard motor are taps (coaxial cables) at turns *1*,*2*,*7*,*8*,*15* and *16* in the first coil from phase *U*; this allowed to measure voltage distribution through this coil.

This is done in this way because voltages between beginning- and final-turns from one phase can be supported since it is usual to have an additional insulation layer between coils in the same phase; moreover, as it was remarked at section 2.1, nearly the whole voltage from the source is displayed in the first coil of the phase.

At the same time, it was used a pulsed voltages generator whose output provided steep fronted waveforms with rise times down to 40ns for different voltage amplitudes. Its output was connected to a snubber circuit in order to slow down *du/dt* values and study turn by turn voltage propagation for different rise time values.

In these experiments, it was compared voltage distributions with the phase terminal connection grounded (see Figure 3.22) and ungrounded (see Figure 3.23). The final experimental setup can be seen at Figure 3.24.

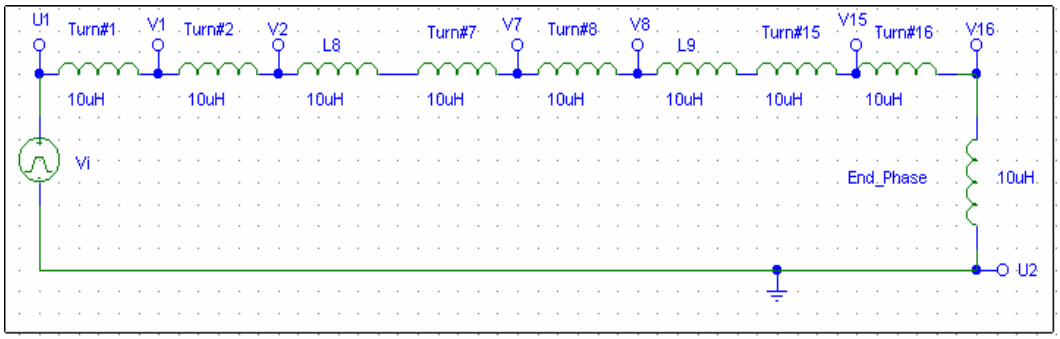

Figure 3.22.- Experimental setup. Configuration for *U2* grounded.

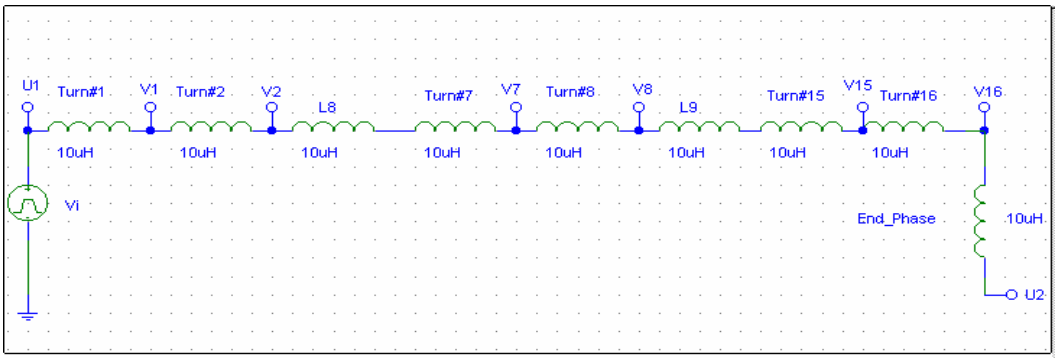

Figure 3.23.- Experimental setup. Configuration for *U2* ungrounded.

Figure 3.24.- Complete experimental setup.

3.6.2.- Experimental results.

In this section, results from turn by turn voltage propagation through stator coils are presented for 2.4μs, 320ns, 120ns y 40ns rise times. Maximum turn to turn voltages are greater as rise times are lower (see Table 3.5).

Rise time	2400 ns	320 ns	120 ns	40 ns
Maximum voltage between turns #7 and #16	28 V	40 V	60 V	72 V
Maximum voltage between turns #1 and #8	16 V	24 V	32 V	40 V
Maximum voltage between turns #1 and #16	40 V	56 V	80 V	92 V

Table 3.5.- Maximum turn to turn voltages for different rise times.

Voltage propagation results were compared to those with the phase terminal connection openopen circuited and it could be seen that transient voltage distribution is similar in both cases, but different for greater periods of time (see Figures 3.35-3.40) as expected from the theoretical steady state behaviour. Impedance mismatch differences explain v_{16} behaviour after 1.6μs in both configurations.

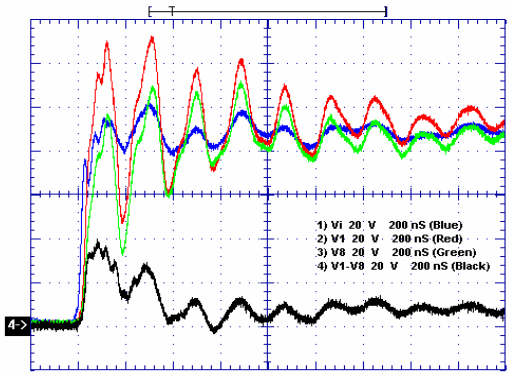

Figure 3.35.- Input voltage (blue), at turns #1 (red), #8 (green) and between turns #1 and #8 (black). Rise time 40ns. *U2* grounded.

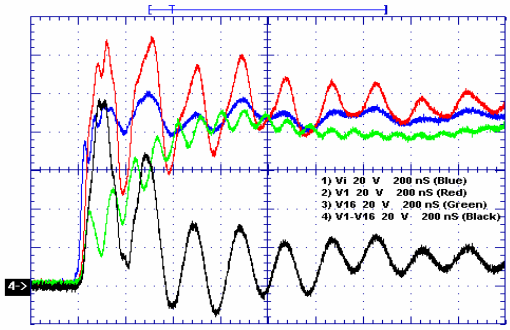

Figure 3.36.- Input voltage (blue), at turns #1 (red), #16 (green) and between turns #1 and #16 (black). Rise time 40ns. *U2* grounded.

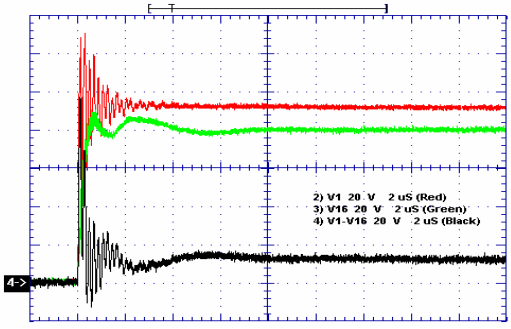

Figure 3.37.- Voltage at turns #1 (red), #16 (green) and between turns #1 and #16 (black). Rise time 40ns. Reaching steady state. *U2* grounded.

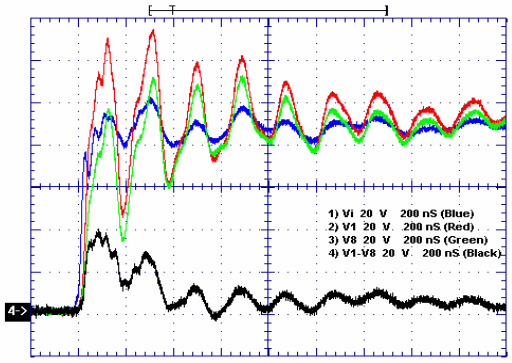

Figure 3.38.- Input voltage (blue), at turns #1 (red), #8 (green) and between turns #1 and #8 (black). Rise time 40ns. *U2* ungrounded.

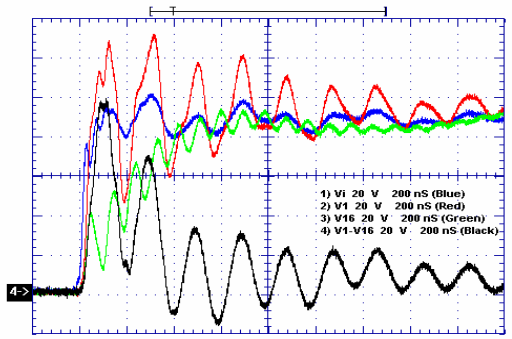

Figure 3.39.- Input voltage (blue), at turns #1 (red), #16 (green) and between turns #1 and #16 (black). Rise time 40ns. *U2* ungrounded.

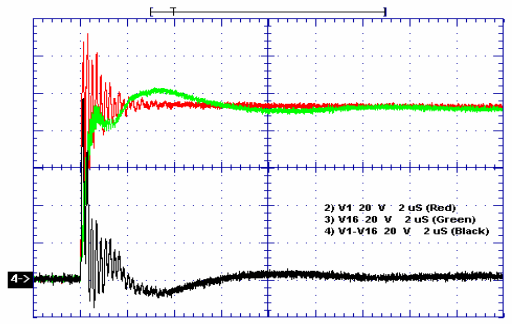

Figure 3.40.- Voltage at turns #1 (red), #16 (green) and between turns #1 and #16 (black). Rise time 40ns. Reaching steady state. *U2* ungrounded.

3.6.3.- Discussion.

Measurements confirm the existence of high turn to turn voltages across one coil into a winding, and magnitude growing with lower rise times (see Figure 3.42). Moreover, for steep fronted transients high enough it can be observed how the whole input voltage is developed between firsts and lasts turns from the coil (see Figure 3.36). Thus, it seems to be very important to calculate possible electrical stresses that may appear at firsts and lasts turns into each phase's first coils in stator windings because they may undergo repetitive greater voltages.

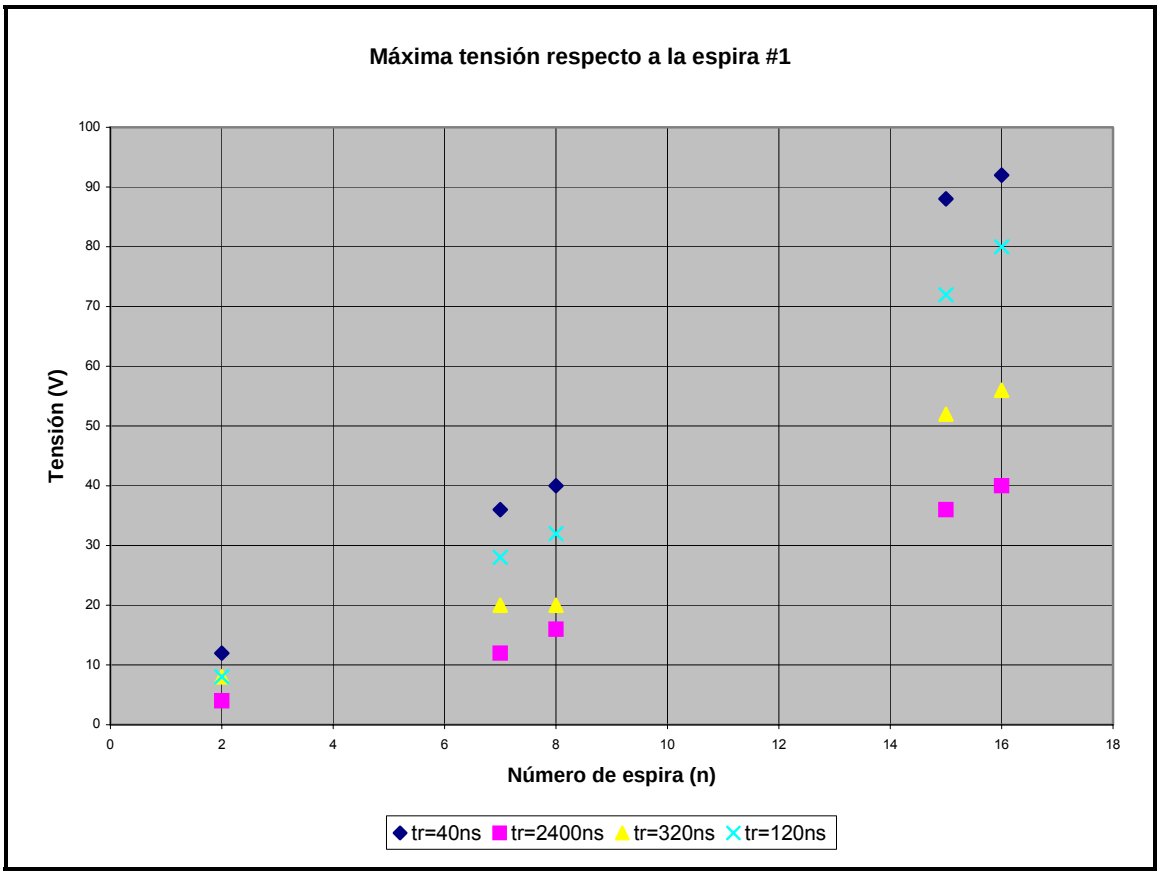

Figure 3.42.- Maximum turn #*n*-turn #*1* voltages for different rise times (*tr*).

3.7.- Conclusions.

In this chapter it was presented a model for turn by turn voltage calculation through random wound coils. When using appropriate hypothesis, the model –that solves equations in the frequency domain- was initially applied to a coil with a reduced number of turns. Its reliability was proven into several random wound coils by means of impedance measurements made just in one coil. This methodology was used to study the influence that certain equivalent circuit parameters have on its accuracy, in order to justify some

approximations. Finally, a turn by turn voltage propagation analysis made on a real induction motor subjected to steep fronted pulses remarks that voltages at firsts and lasts turns in the coil are those that need more attention regarding to electrical stresses prediction. These issues are necessary in order to solve problems faced in the following chapter.

4.- Voltage calculation and analysis through real coils.

4.1.- Introduction and Objectives.

In this chapter the previously described model will be applied to a real coil inserted in an electrical machine stator. Direct application of this model to a random wound coil with higher number of turns leads to a set of too many equations excessively complex. It is more interesting to apply the same methodology to a winding with taps just in the most critical points in the coil: firsts and lasts turns of the coil. Despite experimental setup will be different, some of the parameters measurements and approximations will be similar to those of chapter three. This will allow an accurate voltage calculation through random wound coils with high number of turns in the frequency domain. Once model reliability is confirmed, the approach of neglecting some electrical parameters from the equivalent circuit will be studied too.

Information contained in frequency domain voltage calculation will be used to compute time domain response of the coil subjected to a voltage pulse whose rise time is similar to inverters'; this can be done by means of iFFT. This will be used to calculate turn by turn voltage propagation through coils subjected to steep fronted pulses of the same magnitude and shape as those present in industrial environments.

4.2.- Experimental setup and winding electrical parameters.

On a conventional induction motor stator, a 49 turns coil was wound in a random way with electrically accessible winding taps. In fact, a 44 turns coil was wound and other 5 turns were superimposed to it. In this way, once all turns will be linked, a 49 turns coil with taps at the first 2 and the last 3 turns will be available (see Figure 4.2). Previously, in the same way as in chapter three, all the impedances from the coil were measured in order to characterize the whole winding; in this particular case, central 44 turns coil impedance had to be measured as well. The remaining approximations used to properly specify equivalent circuit parameters (proximity effect, mutual inductances…) are the same as explained in chapter three.

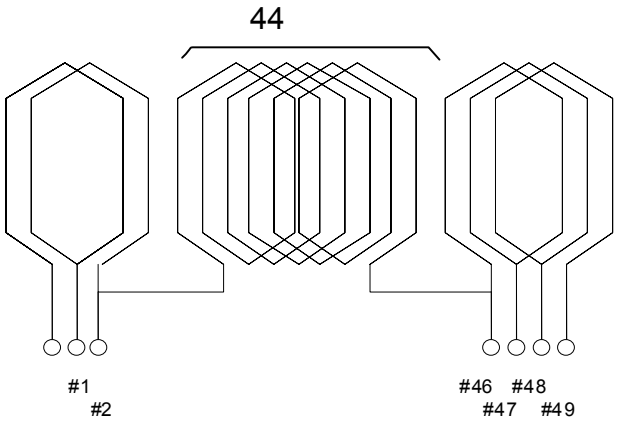

Figure 4.2.- Measurement taps distributed through the coil.

4.3.- Analytical approach to the equivalent circuit in the frequency domain.

4.3.1.- Configuration 1: Feeding between coil input and ground.

This configuration is interesting in order to analyse turn by turn voltage distribution when the winding final connection is an open circuit that may lead to a complete reflection phenomenon in the voltage wave propagation.

Applied methodology is the same as that presented in the previous chapter but with the distinction of considering the central 44 turns winding as a single cell modelled in lumped parameters. After applying the mesh method to calculate all stray currents, each turn to ground voltage for all frequencies under study is obtained by means of the corresponding impedance values.

The results from running the model are presented at Figures 4.5-4.8, and they are compared to experimental measurements for all frequencies and taps in the same way as in section 3.5. There is a great agreement between experimental and theoretical approaches both in amplitude and phase for each voltage studied in this high frequency ranges.

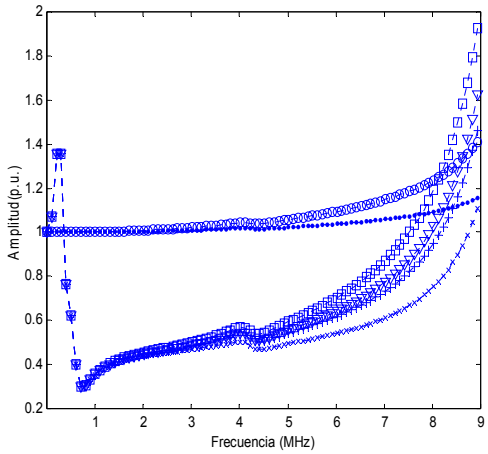

Figure 4.5.- Voltage amplitude at turns #1(●), #2 (❍), #46 (X), #47 (+), #48 (▽) and #49 (□). Results corresponding to the theoretical model.

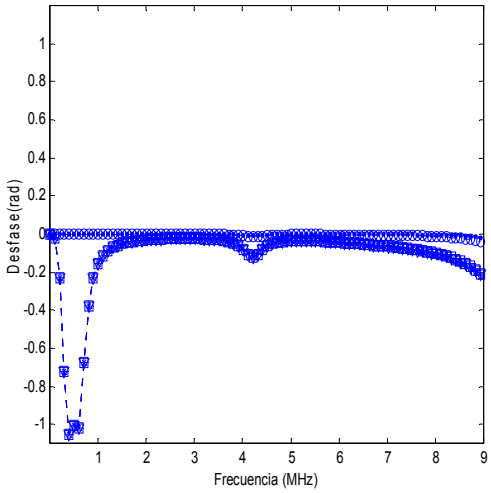

Figure 4.6.- Voltage phase at turns #1(●), #2 (❍), #46 (X), #47 (+), #48 (▽) and #49 (□). Results corresponding to the theoretical model.

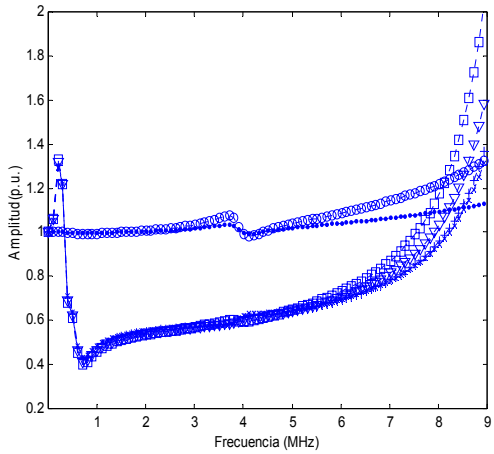

Figure 4.7.- Voltage amplitude at turns #1(●), #2 (❍), #46 (X), #47 (+), #48 (▽) and #49 (□). Experimental results.

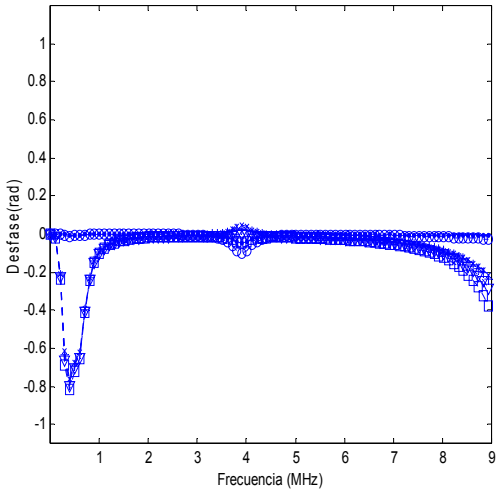

Figure 4.8.- Voltage phase at turns #1(●), #2 (❍), #46 (X), #47 (+), #48 (▽) and #49 (□). Experimental results.

4.3.2.- Configuration 2: Feeding between both coil terminals.

This configuration has been used in order to study voltage propagation in a wye-connected motor subjected to high *dU/dt* values. Despite two phases are connected in series during the transient voltage, for the short periods of time that this work is studying, nearly the whole applied voltage transient falls in its first coil.

As in previous section, it will be applied the same methodology as in chapter 3 in order to calculate turn by turn voltage distribution through this random wound coil. Central 44 turns coil will be modelled in the equivalent circuit by using lumped parameters.

As can be seen from Figures 4.11 and 4.12, theoretical turn to turn voltage calculation is very close, to the high frequency voltage measurements made through the winding. Moreover, equivalent winding impedance calculated by the model have the expected frequency dependence behaviour, both for resistance and reactance (see Figures 4.13 and 4.14); in addition to this, this calculations are in good agreement with overall coil measured impedance.

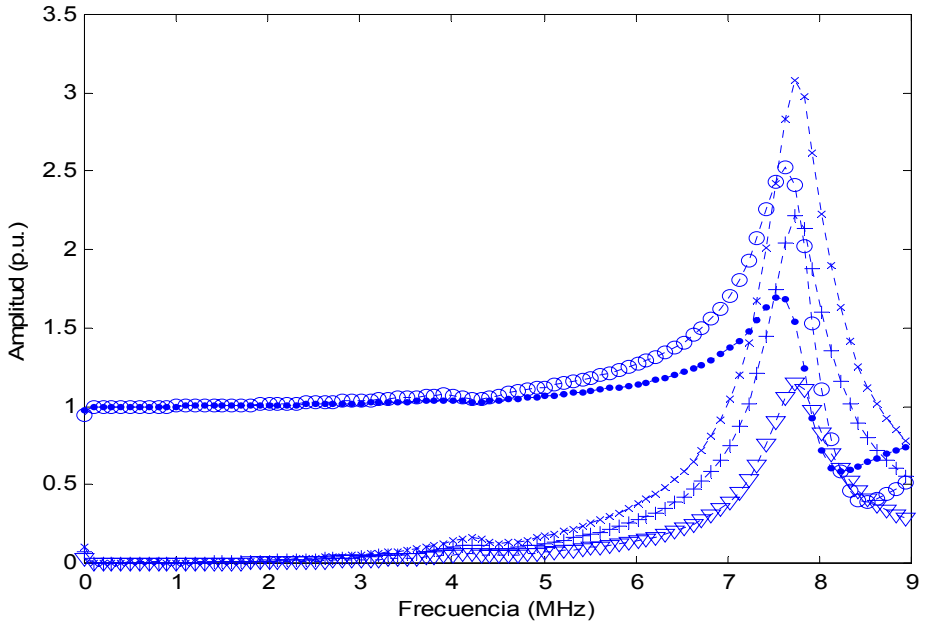

Figure 4.11.- Voltage amplitude at turns #1(●), #2 (❍), #46 (X), #47 (+) and #48 (▽). Results corresponding to the theoretical model.

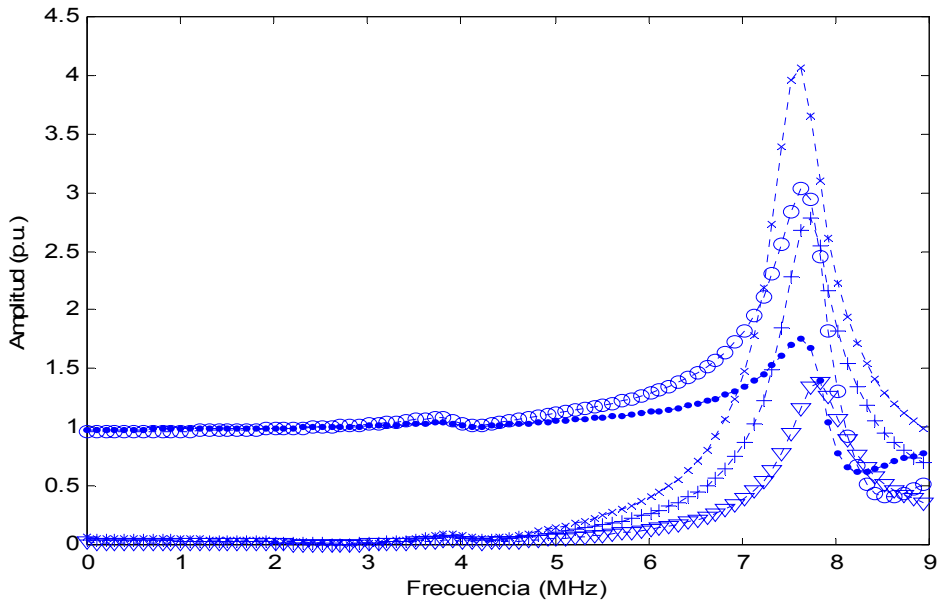

Figure 4.12.- Voltage amplitude at turns #1(●), #2 (❍), #46 (X), #47 (+) and #48 (▽). Experimental results.

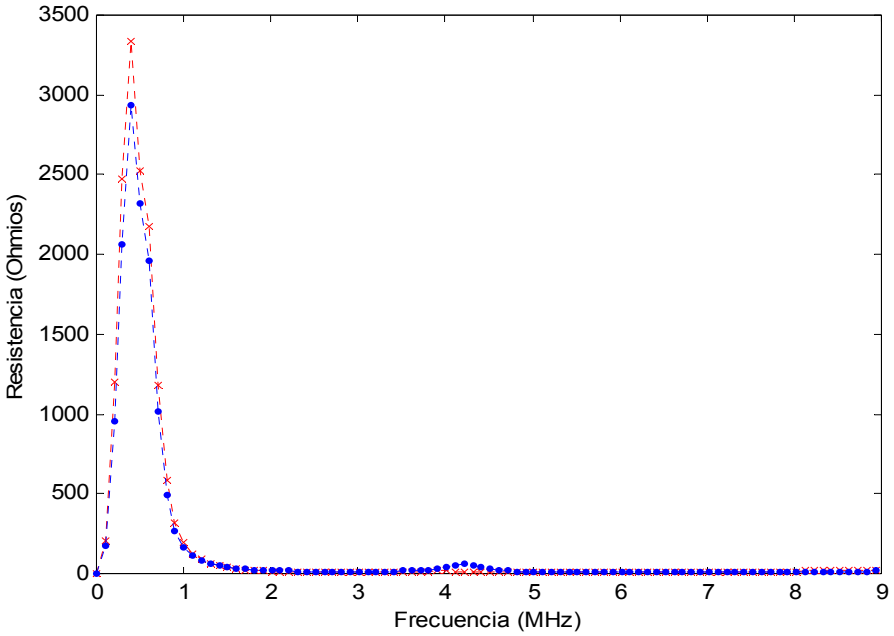

Figure 4.13.- Experimental (x) and theoretical (●) coil resistance data.

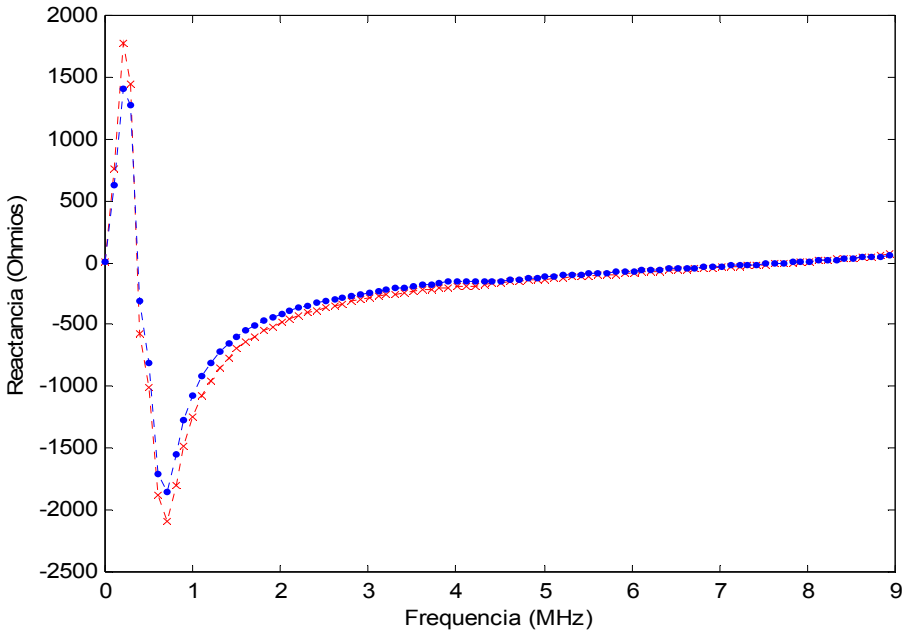

Figure 4.14.- Experimental (x) and theoretical (●) coil reactance data.

4.3.3.- Model validation for different approximations with electrical parameters.

As it was done in the previous chapter with five-turns coils, in this section it will be studied the voltage calculation capability of the model when different approximations were made in its electrical parameters. Mean accumulated absolute errors defined at section 3.5.3 were used as the parameters to quantify deviations from experimental measurements. The study was made for both winding configurations described previously.

It is clear from the analysis made (see Tables 4.1 and 4.2), that neglecting dielectric losses from the equivalent circuit does not affect voltage calculation. In opposition to this, neglecting proximity and skin effects has a negative effect into voltage prediction, specially in phase calculation. On the contrary, it is voltage amplitude calculation which is more difficult when neglecting mutual inductances. All these results are in agreement with those extracted from section 3.5.4.

Model	**Amplitude error (p.u.)**	**Phase error (rad)**
Complete	0.0587	0.0297
Neglecting losses due to skin and proximity effect.	0.1009	0.4592
Neglecting mutual inductances	0.0803	0.0296
Neglecting either mutual inductances and losses due to skin and proximity effect	0.0932	0.4509

Table 4.1.- Mean accumulated absolute errors (amplitude and phase) for each model Configuration 1: Feeding between coil input and ground.

Model	**Amplitude error (p.u.)**	**Phase error (rad)**
Complete	0.0673	0.4148
Neglecting losses due to skin and proximity effect.	0.2255	1.8019
Neglecting mutual inductances	0.1225	0.4456
Neglecting either mutual inductances and losses due to skin and proximity effect	0.2042	0.5681

Table 4.2.- .- Mean accumulated absolute errors (amplitude and phase) for each model Configuration 2: Feeding between both coil terminals.

4.4.- Time domain prediction.

4.4.1.- Objectives and methodology.

The model proposed in the previous section allows to make turn by turn transfer functions calculation $\boldsymbol{H_k(\omega)}$ when the applied voltage is $\boldsymbol{U(\omega)}$. In this section, the whole information contained in these transfer functions in the frequency domain, was used in order to calculate turn by turn time domain voltages $u_k(t)$ for both studied configurations when the coil is subjected to steep fronted pulses $u(t)$ with rise times similar to those found in actual frequency converters (see Figure 4.15). In order to accomplish with this task, direct and inverse Fast Fourier Transform (iFFT) were used. In addition to the comparison in voltage prediction by means of experimental and theoretical transfer functions, some direct measurements were made along all taps in the winding when fed by a real signal with similar amplitude and rise time values than that used for the Fourier transformation (see Figure 4.17).

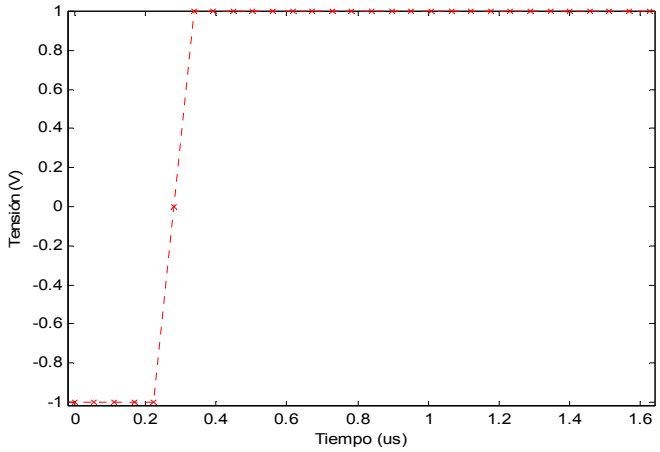

Figure 4.15.- Winding input voltage ($u(t)$) used for time domain calculation model.

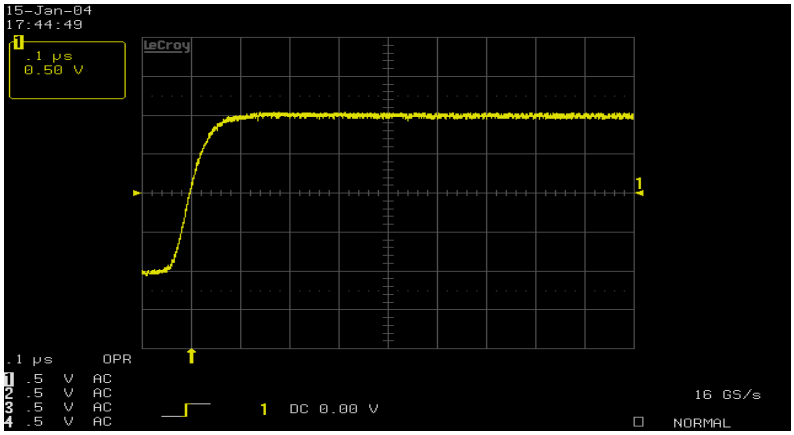

Figure 4.17.- Winding real input voltage used for direct measurements along the coil.

4.4.2.- Model validation in voltage distribution calculation.

Firstly it is necessary to calculate frequency domain voltages in each winding turn *k* for the previously described feeding voltage *u(t)*. This is the reason of using the following equation:

$$U_k(\omega) = H_k(\omega) * U(\omega)$$

(4.11)

where $\boldsymbol{U(\omega)=fft(u(t))}$. In order to make the necessary transformations it is convenient to have $\boldsymbol{H_k(\omega=0)}$ data and taking into account that the maximum time step that must be used to apply FFT correctly is $\Delta t = 1/(2 * f_+)$ by means of the sampling theorem. This new time domain sensitivity value must be applied to $\boldsymbol{U(\omega')}$ in order to have this signal with a frequency spectrum coherent to it; this new spectrum is usually different from that of the transfer functions $\boldsymbol{H_k(\omega)}$, so it is necessary to redefine them interpolating data from both frequency spectrum. Finally, the time domain winding response to this steep fronted transient *u(t)* for each coil turn *k* can be calculated, just by applying iFFT to $\boldsymbol{U_k(\omega')}$. All these results will be compared to direct experimental measurements along the coil, as presented in the resume depicted in Figure 4.18.

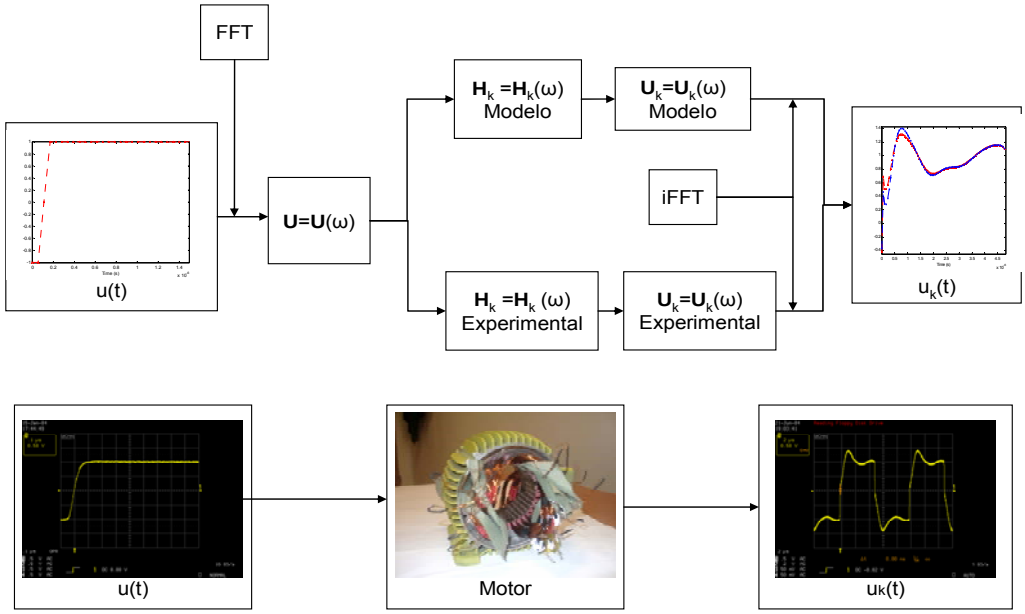

Figure 4.18.- Sketch-resume of applied methodology.

4.4.2.1.- Configuration 1: Feeding between coil input and ground.

When using this methodology for both transfer functions, it can be easily observed a great coincidence between theoretical and experimental calculations for all turns (see, for example, Figure 4.19). The validation of this methodology can be remarked by comparing voltage distribution calculation made in both ways with direct measurements made through the winding fed with steep fronted transients waveshapes similar to *u(t)* (see Figures 4.23).

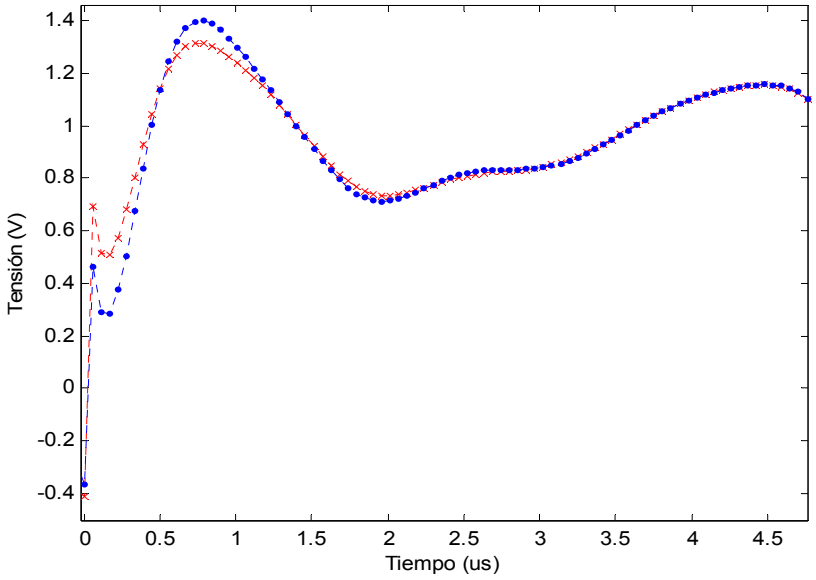

Figure 4.19.- Theoretical (●) and experimental (x) time domain voltage at turn #46.

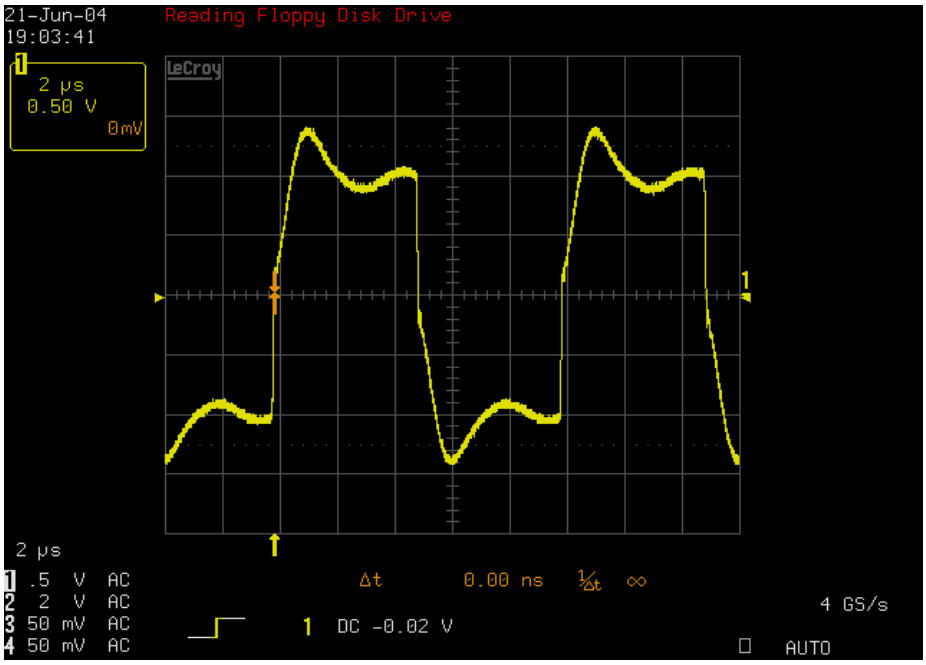

Figure 4.23.- Voltage direct measurement at turn #46.

Bandwidth limitations in winding characterization and some approximations made (frequency interpolation, used feeding signals are not exactly equal…) explain some slight differences in the first periods of time between transfer functions calculations and direct measurements. Despite this, the times when maximum electrical stresses are present (1.2µs y 4.4µs), and its own magnitudes (1.4V and 1.1V) are very close in both cases for all nodes.

The overvoltage that arises in the final turns of the coil is due to its open circuited final terminal leading to reflection phenomena.

4.4.2.2.- Configuration 2: Feeding between both coil terminals.

Maximum turn to turn calculated voltages and the times when they appear, are in good agreement with those from measured waveshapes (see Figures 4.27-4.32).

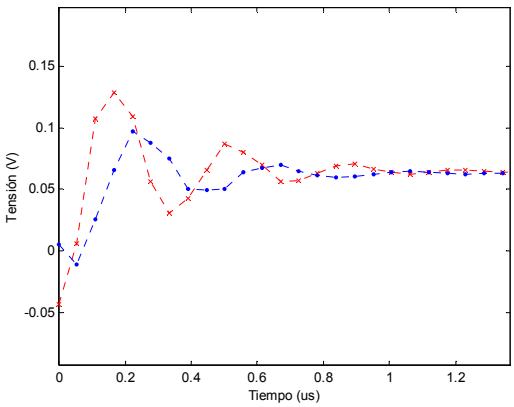

Figure 4.27.- Theoretical (●) and experimental (x) time domain voltage at turn #46.

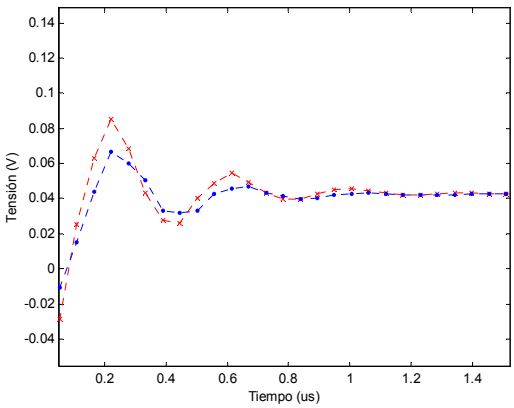

Figure 4.28.- Theoretical (●) and experimental (x) time domain voltage at turn #47.

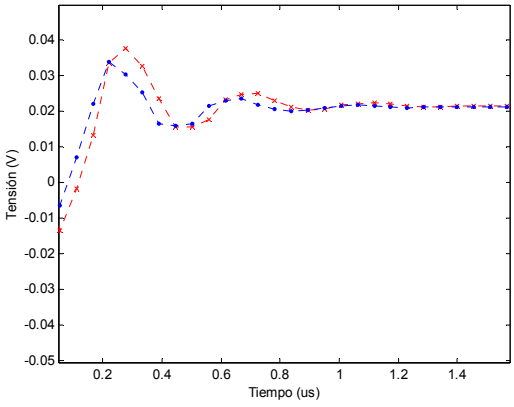

Figure 4.29.- Theoretical (●) and experimental (x) time domain voltage at turn #48.

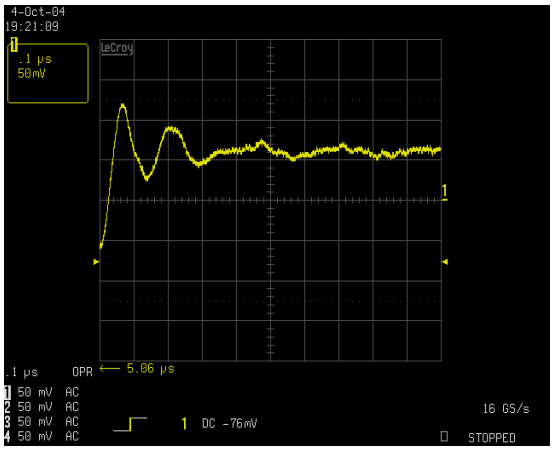

Figure 4.30.- Voltage direct measurement at turn #46.

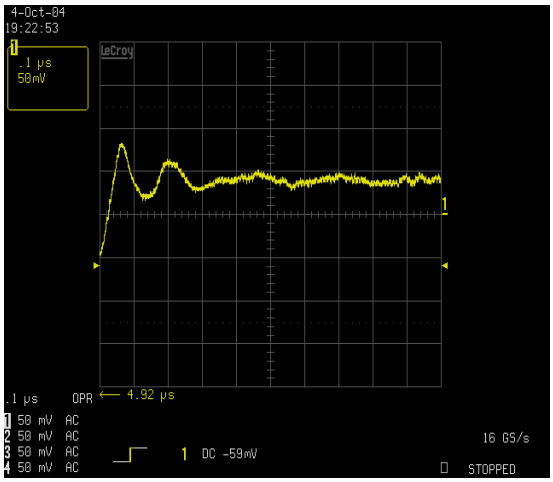

Figure 4.31.- Voltage direct measurement at turn #47.

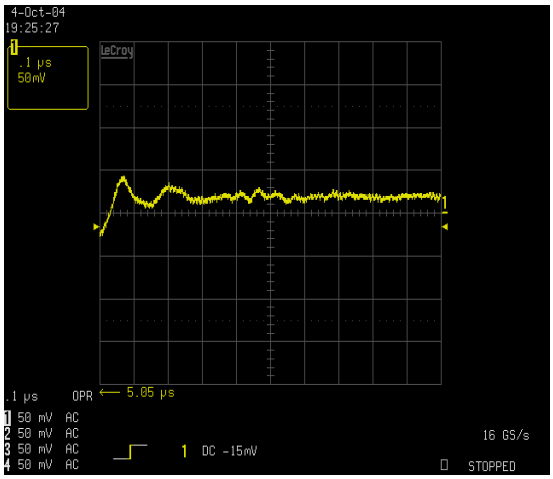

Figure 4.32.- Voltage direct measurement at turn #48.

4.4.3.- Model extension to voltage distribution calculation with different feeding pulses.

After model efficiency confirmation, it was applied to analyze turn by turn voltage propagation through the coil in both winding configurations when it was subjected to transient voltages with similar *du/dt* values as presented in real industrial environments (see Figure 4.33). When the model was applied in configuration 2, it was observed that the whole voltage does not only falls between first and last turns, but also between any of the firsts and lasts turns (see Figures 4.35 and 4.36), so it is fairly possible that just the enamel thickness would be the only insulation protection versus these high amplitude impulses.

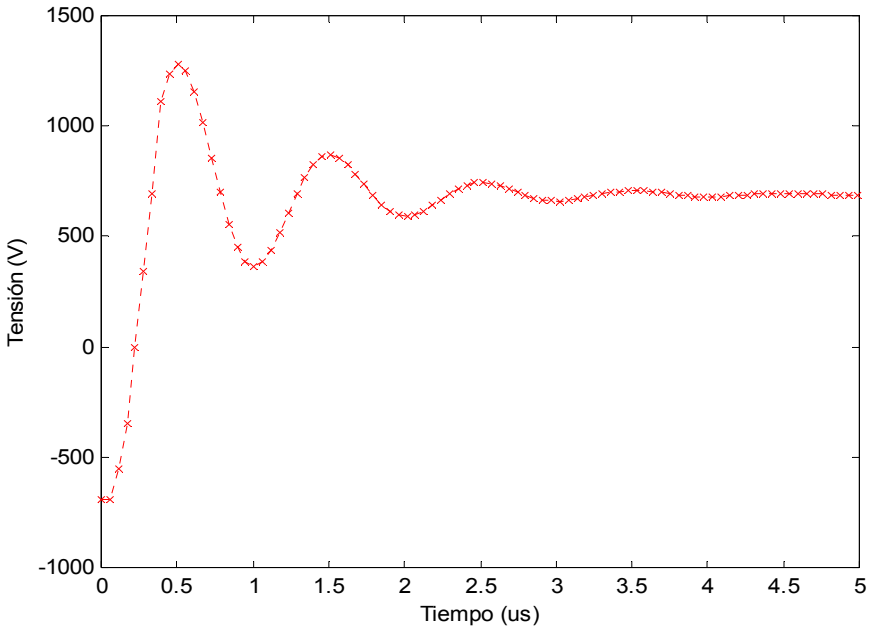

Figure 4.33.- Winding input voltage (*u(t)*) used for time domain calculation model.

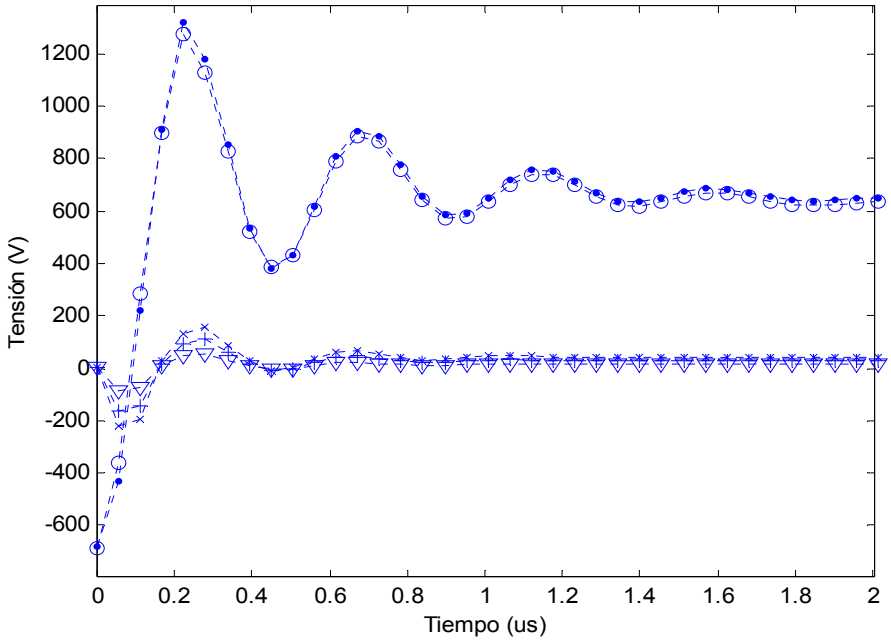

Figure 4.35.- Voltage distribution calculation through turns #1(●), #2 (❍), #46 (X), #47 (+) and #48 (▽) using the model at configuration 2.

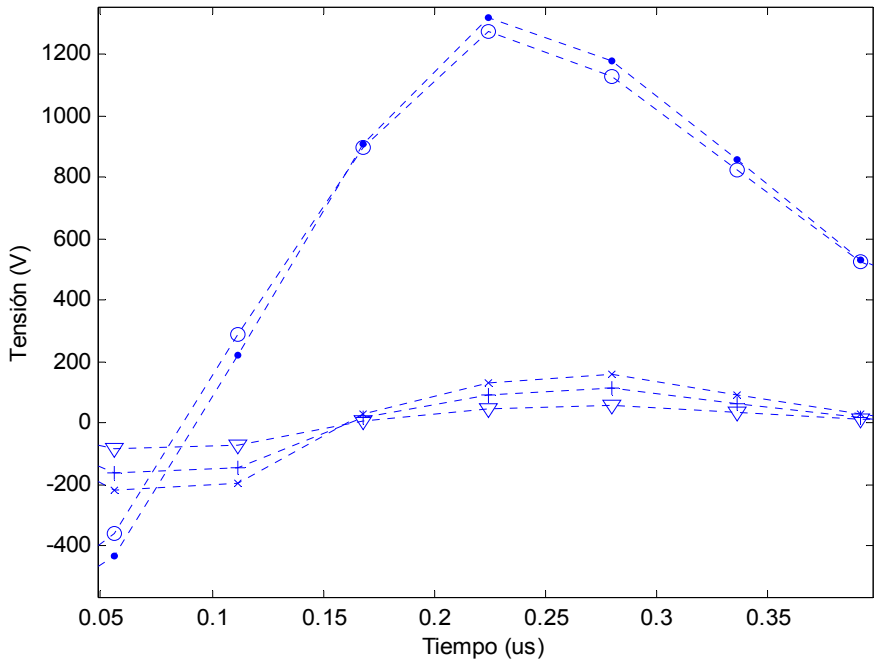

Figure 4.36.- Voltage distribution calculation through turns #1(●), #2 (❍), #46 (X), #47 (+) and #48 (▽) using the model at configuration 2. Zoom..

4.5.- Conclusions.

Using the results from chapter 3 it has been possible to apply the same methodology to voltage calculation through a coil with high number of turns inserted in a real motor stator in the frequency domain. By comparison with experimental measurements, it can be seen that the model calculates reliably voltage amplitudes and phases for both configurations under study (final coil terminal floating or connected to source's ground) through a reduced number of winding impedance measurements. The application of this model confirms conclusions from the previous chapter about the effect that some approximations made on the equivalent circuit have on its accuracy.

Finally, FFT was applied to calculate turn by turn voltages in the time domain by using frequency domain data. Results from model execution for both configurations were compared not only with those from the experimental transfer functions, but also with direct turn by turn voltage propagation measurements through the coil. In addition to this, the model was applied in order to calculate internal voltage distribution through the coil subjected to voltage pulses similar to those found in industrial environments, and this allowed to notice the presence of critical points inside it.

5.- Industrial applications of the model into impregnated coils: Ageing Indication.

5.1.- Introduction and Objectives.

In low voltage motors, coils inserted in slots are usually varnished, so in this chapter the frequency domain calculation model presented in chapter 3 was firstly applied to varnished coils using different kinds of resins. Afterwards, impedance measurements from a non impregnated coil have been used to calculate voltage distribution in impregnated ones just taking into account changes in stray equivalent capacitances. Finally, after checking how voltage distribution was affected by turn-to-turn and turn-to-ground capacitances, their values were changed in order to achieve a more even voltage distribution through the coil.

Since it is clear that PD is a main cause of insulation ageing by means of turn-to-turn insulation degradation, in this chapter accelerated PD ageing processes have been applied to these turn-to-turn insulation systems in random wound coils. In addition to study the ageing process in different varnishes, it has been proposed new techniques to achieve dielectric status diagnosis.

5.2.- Impregnation process and experimental methodology.

5.2.1.- Mould description.

In order to allow the curing process to take place, it is necessary to have a setup that allows different mixtures resin/hardener injection, have an easy geometry and an easy disassembly. The chosen mould has a *U* shape with six channels for the turns' input and output (see Figure 5.1).

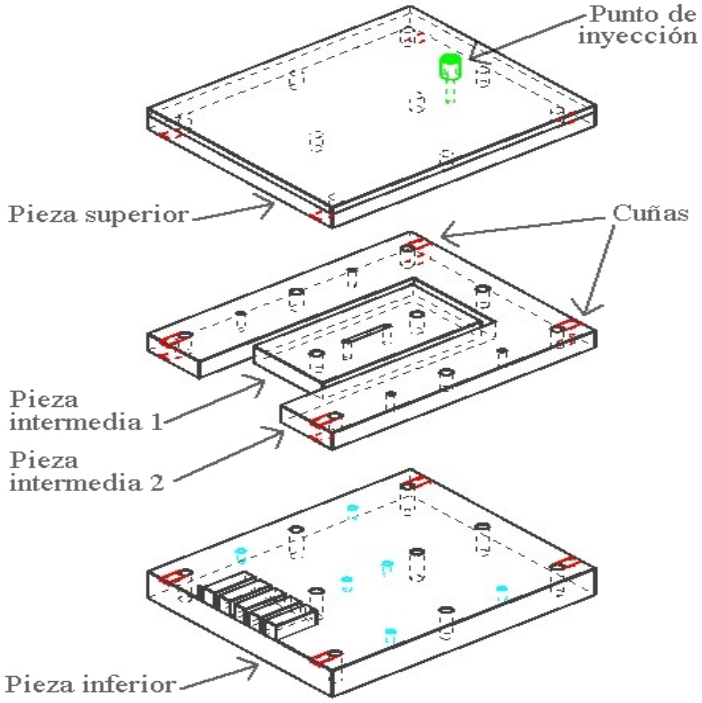

Figure 5.1.- Sketch for the mould used for impregnation.

5.2.2.- Coil winding.

Firstly it is necessary to spread a non-adherent component along all the mould pieces, channels (slots), and inside the injection point, in order to allow varnished coil extraction. Afterwards, pieces 1 and 2 are joined (see Figure 5.2), so magnet wire can be wound around. The process and wire characteristics are the same as in chapter 3. Output channels allow having electrical access to the five-turns coil (see Figure 5.3).

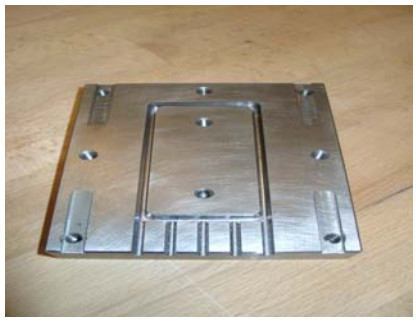

Figure 5.2.- Lower piece adjusted to pieces 1 and 2.

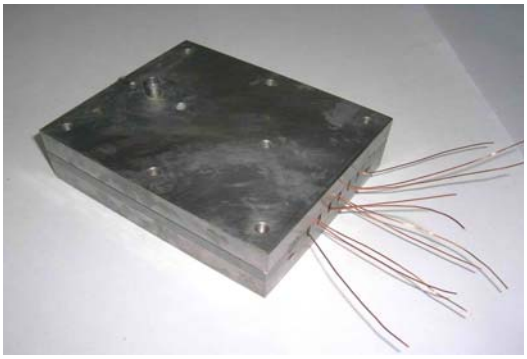

Figure 5.3.- Coil inside the mould.

5.2.3.- Sample impregnation, curing and extraction.

Resin-hardener mixtures were made following the conditions shown in Table 5.1. Before and after varnish injection, its gas content was reduced using vacuum line; this contributed to void content reduction within the dielectric. The use of non-adherent components and wedges located between pieces allow sample extraction from the mould without breaking it.

Sample	***Epoxi equivalent weight***	***Resin/hardener ratio***	***Curing conditions***	***Post-curing conditions***
Impregnated coil #1 (Royapox+Isoforondiamine)	208 gr/eq	1 gr/0.4 gr	100ºC – 4h	-
Impregnated coil #2 (HDGEBA+PAMS)	210 gr/eq	1 gr/0.28 gr	90ºC – 1h	120ºC – 1h

Table 5.1.- Mixture-Curing conditions for both varnishes.

5.2.4.- Resin-Hardener description.

First case under research (*Impregnated Coil #1*) was a commercial varnish used as insulation in low voltage motors: *ROYAPOX 5050* epoxi resin from *S.E.G. ROYAL DIAMOND Inc.*. It has good resistance to moisture penetration and excellent mechanical and dielectric properties. Other characteristics from this resin are:

Viscosity (25ºC): 4000±1000 mPA.s
Density (20ºC): 1.15±0.01 grs/cm^3.

Hardener 5050, provided from the manufacturer, is a compound from Isophorondiamine with the following characteristics:

Viscosity (25ºC): 30±10 mPA.s
Density (20ºC): 0.99±0.02 grs/cm^3

In order to verify model reliability for different materials, it was used a synthetic varnish chosen by the Material Science Department from Universidad Carlos III of Madrid due to its thermal and electrical properties. After the impregnating-curing process described at Table 5.1, a new five-turns varnished coil was available (*Impregnated Coil #2*). The resin is HDGEBA, provided by *CVC Specialty Chemicals Inc*., whose chemical structure is based on an hydrogenized derivation from DGEBA (diglicidilether from bisphenol A, more information at [Pascault, 2002]) molecule but with saturation in its rings. Its commercial name is EPALLOY 5000 and its main characteristics are:

Viscosity (25ºC): 1300±10 mPA.s
Density (20ºC): 0.89±0.01 gr/cm^3

At the same time, the associated hardener PAMS (poly(3-aminopropilmetilsiloxane)) was made at the laboratory following the synthetic procedure shown at [Cabanelas, 2001].

5.2.5.- Final Result.

After all this process, impregnated coils as the one presented in Figure 5.5, were available. Frontal taps allow measuring impedances for equivalent circuit definition and turn by turn transfer functions to check model accuracy.

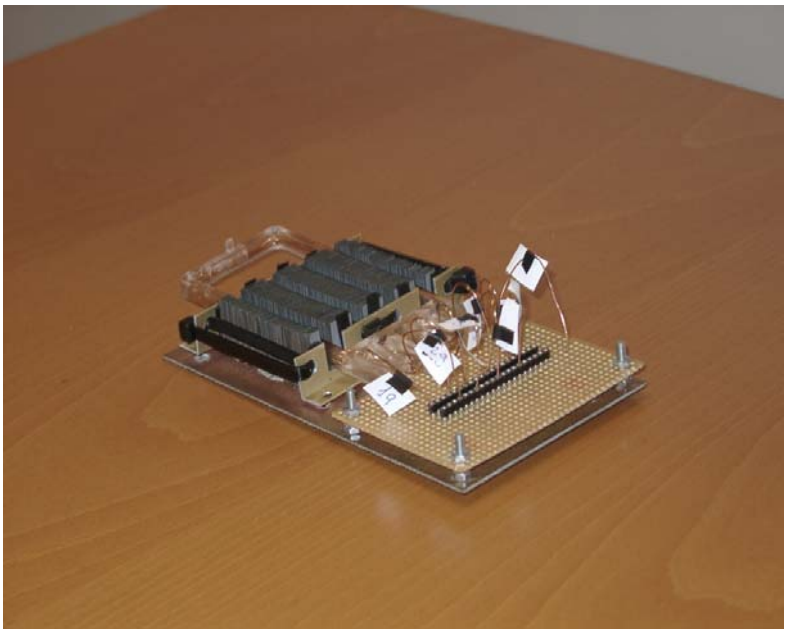

Figure 5.5.- Five-turn varnished coil..

5.3.- Voltage distribution calculation.

5.3.1.- Model application to impregnated coils.

Voltage distributions were studied for three different cases: coil without varnish, impregnated coil #1 and #2. To achieve this objective, the frequency domain model presented in chapter 3 was applied to the three samples, and calculated voltages were compared to experimental measurements. In order to quantify the comparisons, mean accumulated absolute errors defined at section 3.5.3 were used again for each sample. From the results presented in Table 5.2, it is clear that the model is able to calculate accurately turn by turn voltage distribution in a high frequency range in impregnated coils as well.

Sample	Amplitude error (p.u.)	Phase error (rad)
Non-varnished sample	0.0278	0.0130
Impregnated coil #1	0.0267	0.0115
Impregnated coil #2	0.0284	0.0102

Table 5.2.- Mean accumulated absolute errors (amplitude and phase) for each sample.

5.3.2.- Voltage calculation in impregnated coils using stray capacitances.

In this section, impedance measurements from a non-impregnated coil were used to calculate turn by turn voltage distributions through coils impregnated with different varnishes. In order to achieve this, it was taken into account that the most important change arising in the equivalent circuit from the impregnating process is the change in stray

capacitances values; that is why the only modification from measurements in a non-impregnated coil, is the need of taking turn-to-turn and turn-to-ground capacitance measurements from impregnated coils.

The comparison between theoretical results and experimental data for one coil varnished with a commercial resin (see Figures 5.7-5.10) makes it clear that the model reliably calculates turn by turn voltages. In order to check model extension capability, the same methodology was applied to a coil varnished with our synthetic resin, and mean accumulated absolute errors are used again to quantify the efficiency. As can be seen from the results resumed at Table 5.3, this methodology allows reliable voltage calculations for any varnished coil by means of impedance data from a non-impregnated one just by taking into account the change produced in its stray capacitances.

When experimental voltage distribution was analysed for coils with and without impregnation, it is observed how it is more uneven for the latter, as high frequency amplitude and phase harmonics are slightly higher in this case (see Figures 5.9-5.12). In the impregnated coil case, as turn-to-turn equivalent capacitance is bigger than turn-to-ground one, this seems to develop a positive effect on voltage distribution through the coil. Thus, stray capacitances within the coil are verified as main factors in turn by turn voltage distribution through windings subjected to very fast transient voltages.

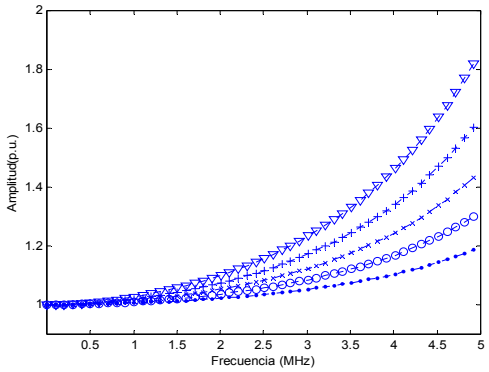

Figure 5.7.- Voltage amplitude at turns #1(●), #2 (❍), #3 (X), #4 (+), and #5 (▽). Results corresponding to the non-varnished theoretical calculation model applied to impregnated coil #1.

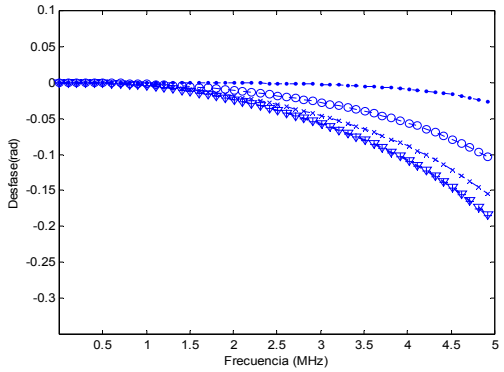

Figure 5.8.- Voltage phase at turns #1(●), #2 (❍), #3 (X), #4 (+), and #5 (▽). Results corresponding to the non-varnished theoretical calculation model applied to impregnated coil #1.

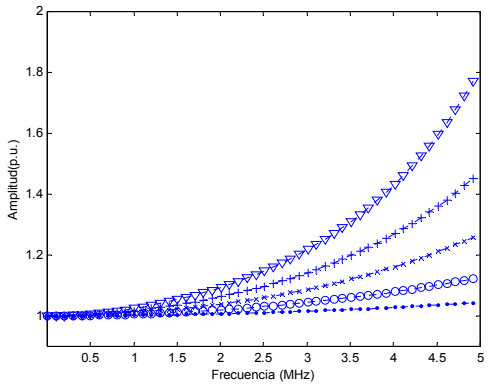

Figure 5.9.- Voltage amplitude at turns #1(●), #2 (❍), #3 (X), #4 (+), and #5 (▽). Experimental results at impregnated coil #1.

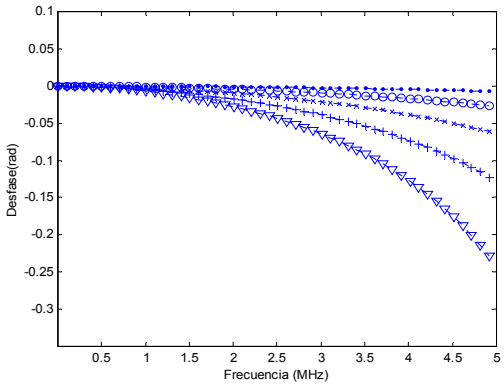

Figure 5.10.- Voltage phase at turns #1(●), #2 (❍), #3 (X), #4 (+), and #5 (▽). Experimental results at impregnated coil #1.

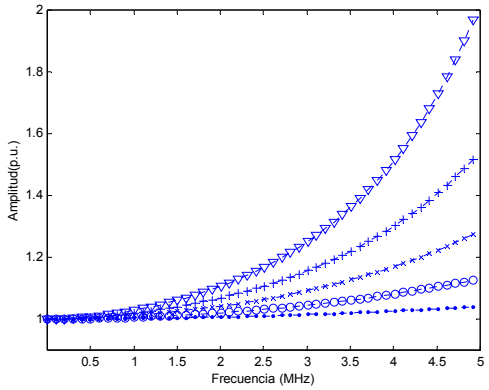

Figure 5.11.- Voltage amplitude at turns #1(●), #2 (❍), #3 (X), #4 (+), and #5 (▽). Experimental results at non-varnished coil.

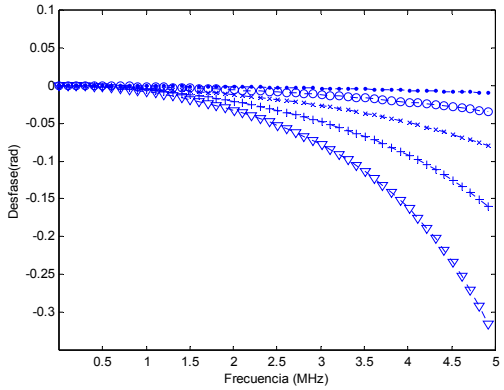

Figure 5.12.- Voltage phase at turns #1(●), #2 (❍), #3 (X), #4 (+), and #5 (▽). Experimental results at non-varnished coil.

Sample	Amplitude error (p.u.)	Phase error (rad)
Impregnated coil #1	0.0353	0.0151
Impregnated coil #2	0.0317	0.0138

Table 5.3.- Mean accumulated absolute errors (amplitude and phase) for each sample using the model and data from the non-varnished coil.

5.4.- Model extension to machine stators.

Since the importance of stray capacitances in voltage distribution has been checked and the model is reliable in its calculus just changing their values, the same methodology of chapter 4 has been applied to the voltage calculation in a 49 turns coil. The aim of this section is to study how changes in stray capacitances values influence voltage distribution for both winding configurations.

Despite the model presented in chapter 4 has proven to be accurate enough, it must be considered that impregnation processes increase turn-to-turn (*Ctt*) and turn-to-ground capacitances (*Ctg*) proportionally to the dielectric constant of the materials involved. As an example, voltage distributions for *Ctt* and *Ctg* values modified in an arbitrary but reasonable way, are compared to electrical stresses from chapter 4 theoretical model. As can be seen in Figures 5.13-5.16, the impregnation process provides more uneven voltage distributions, and hence, greater turn to turn electrical stresses.

In order to solve this, an appropriate winding insulation system has been proposed by means of changing turn-to-turn and turn-to-ground capacitances trying to obtain a more uniform voltage distribution. The results arising from the model application have shown (see Figures 5.17-5.22) that it is convenient that turn-to-turn capacitance should be greater than turn-to-ground one as much as possible in order to get an even voltage distribution. Nevertheless, this asymptotic tendency in voltage distribution is noticeable from *Ctt/Ctg* very high values. The proposal of low *Ctg/Ctt* values in the design of power transformers supposed to undergo classical impulses has been pointed yet ([Dortmont, 1971]), but, up to now, it has not been quantified the variation effect to obtain less aggressive turn-to-turn electrical stresses. These previous models were focused on form wound coils, lower *du/dt* values and did not face experimental validations ([Karsai, 1987], [Jianru, 2002]).

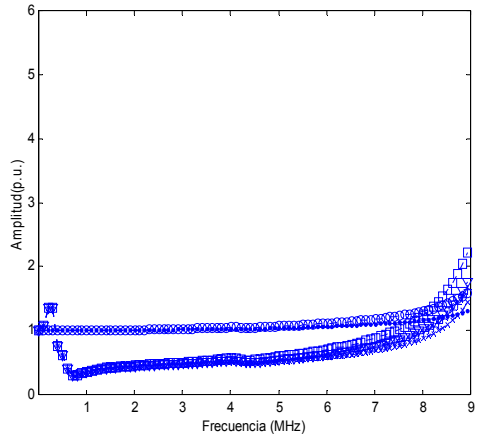

Figure 5.13.- Voltage amplitude at turns #1(●), #2 (❍), #46 (X), #47 (+), #48 (▽) and #49 (□). Results corresponding to the theoretical model applied to configuration 1. Ctt(x1), Ctg(x1).

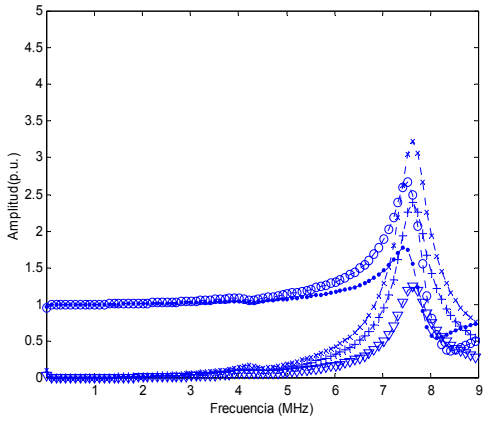

Figure 5.14.- Voltage amplitude at turns #1(●), #2 (❍), #46 (X), #47 (+) and #48 (▽). Results corresponding to the theoretical model applied to configuration 2. Ctt(x1), Ctg(x1).

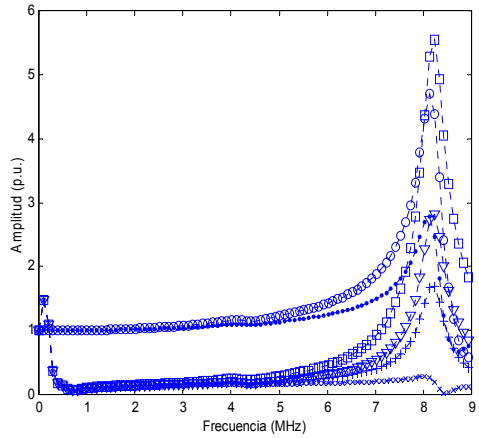

Figure 5.15.- Voltage amplitude at turns #1(●), #2 (❍), #46 (X), #47 (+), #48 (▽) and #49 (□). Results corresponding to the theoretical model applied to configuration 1. Ctt(x3), Ctg(x5).

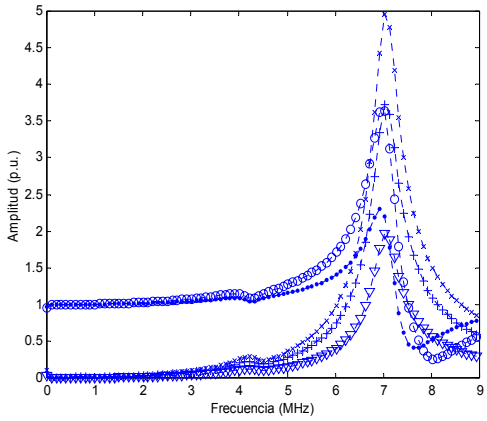

Figure 5.16.- Voltage amplitude at turns #1(●), #2 (❍), #46 (X), #47 (+) and #48 (▽). Results corresponding to the theoretical model applied to configuration 2. Ctt(x3), Ctg(x5).

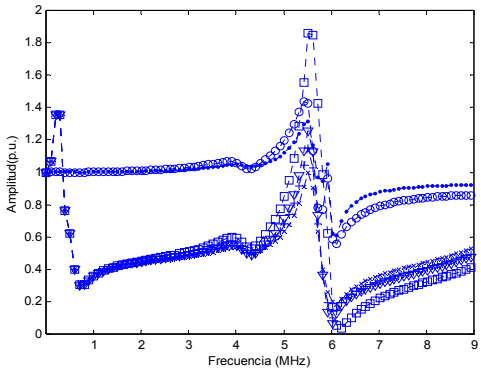

Figure 5.17.- Voltage amplitude at turns #1(●), #2 (❍), #46 (X), #47 (+), #48 (▽) and #49 (□). Results corresponding to the theoretical model applied to configuration 1. Ctt(x100), Ctg(x1).

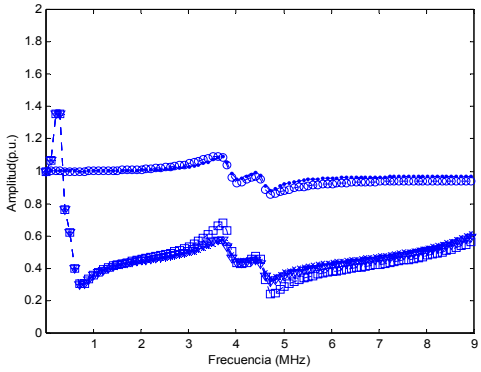

Figure 5.18.- Voltage amplitude at turns #1(●), #2 (❍), #46 (X), #47 (+), #48 (▽) and #49 (□). Results corresponding to the theoretical model applied to configuration 1. Ctt(x200), Ctg(x1).

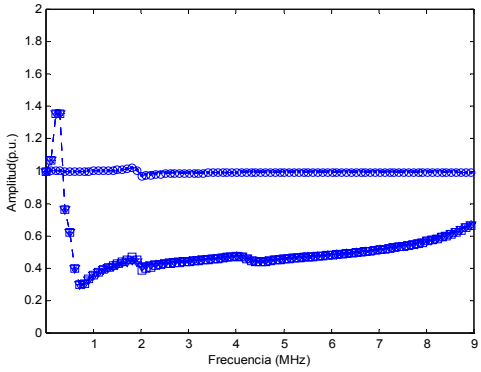

Figure 5.19.- Voltage amplitude at turns #1(●), #2 (❍), #46 (X), #47 (+), #48 (▽) and #49 (□). Results corresponding to the theoretical model applied to configuration 1. Ctt(x1000), Ctg(x1).

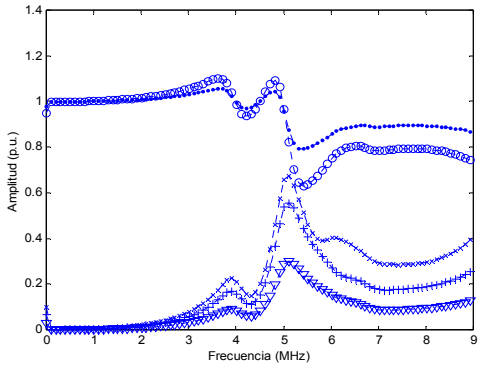

Figure 5.20.- Voltage amplitude at turns #1(●), #2 (❍), #46 (X), #47 (+) and #48 (▽). Results corresponding to the theoretical model applied to configuration 2. Ctt(x100), Ctg(x1).

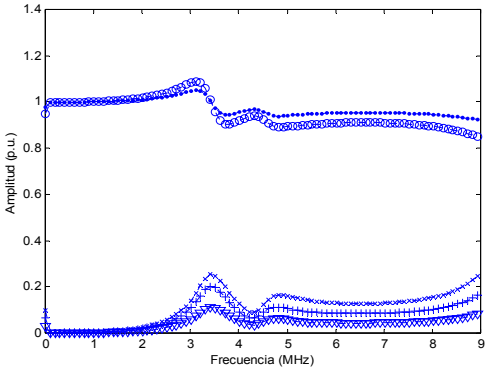

Figure 5.21.- Voltage amplitude at turns #1(●), #2 (❍), #46 (X), #47 (+) and #48 (▽). Results corresponding to the theoretical model applied to configuration 2. Ctt(x200), Ctg(x1).

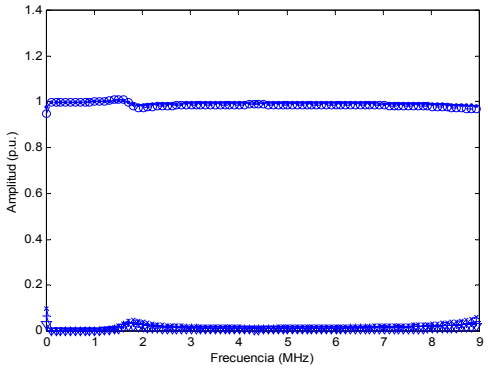

Figure 5.22.- Voltage amplitude at turns #1(●), #2 (❍), #46 (X), #47 (+) and #48 (▽). Results corresponding to the theoretical model applied to configuration 2. Ctt(x1000), Ctg(x1).

5.5.- Turn to turn insulation status characterization after accelerated ageing by partial discharge activity.

5.5.1.- Introduction and experimental setup.

One of the main factors of insulation ageing within these motor coils is PD. This is the reason of studying an ageing indication produced by this process in random wound impregnated coils. In this section it was described the four kinds of varnishes used for ageing studies, whose curing and extraction techniques are similar to those presented in section 5.2:

Samples with Royapox +Isoforondiamine (Material A):	MAi $\forall i \in \{1,2,3,4,5,6\}$
Samples with Royapox + PAMS (Material B):	MBi $\forall i \in \{1,2,3,4,5,6\}$
Samples with DGEBA + PAMS (Material C):	MCi $\forall i \in \{1,2,3,4,5,6\}$
Samples with HDGEBA + PAMS (Material D):	MDi $\forall i \in \{1,2,3,4,5,6\}$

In addition to this, it has been shown the experimental procedure followed in order to avoid premature failures (see Figure 5.26) that do not allow having enough test time to set any ageing tendency.

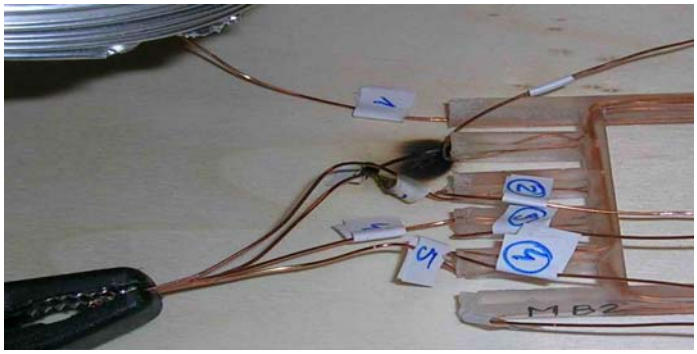

Figure 5.26.- Premature failure due to bad turn selection to connect to test voltage..

In this chapter, a set of impregnated five-turn coils were subjected to accelerated ageing processes by applying sinusoidal voltage levels similar to those reached by inverter fed drives into its turn-to-turn insulation system. Voltages were applied between one turn and all the rest shortcircuited (see Figure 5.24). These electrical stresses provide a high PD activity. These processes were applied to non-impregnated samples as well to study inverse power law accomplishment.

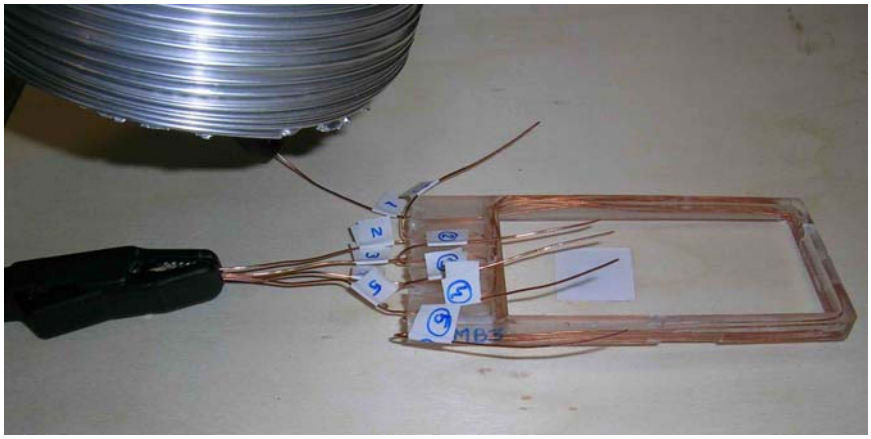

Figure 5.24.- Connection to test voltage.

Certain stop times in ageing processes were chosen in order to record PD activity for the latest 15s in each ageing interval. On this purpose it was used a commercial PD detection system. Afterwards, it was made impedance measurements ($Z=Z(\omega)$) by means of FRA technique; trying to take into account the wider variety of dielectric polarization phenomena, the frequency sweep was made between 30Hz and 30MHz with 20 points per decade.

5.5.2.- Non-impregnated samples. Inverse Power Law.

Non-varnished samples were subjected to voltage levels that provided great PD activity. For each voltage level, insulation system times to failure were noted in order to have enough statistical data for a time to breakdown versus applied voltage representation ([IEC 60505, 2004]). As can be seen from Figure 5.27, graphical representation of these data and correlation coefficient from least squares regression ($r = -0.9619$) show an appropriate accomplishment of inverse power law presented by other authors as an ageing estimation for electrical stresses:

$$t_b = t_{b0} * U^n \qquad (5.1)$$

Despite there are some similar experimental results from other works ([Fabiani, 2003]), main differences with other author's data ([Lebey, 1998], [Manz, 1997]) are due to differences in applied voltage magnitude, material and thickness of tested enamel and kind of sample.

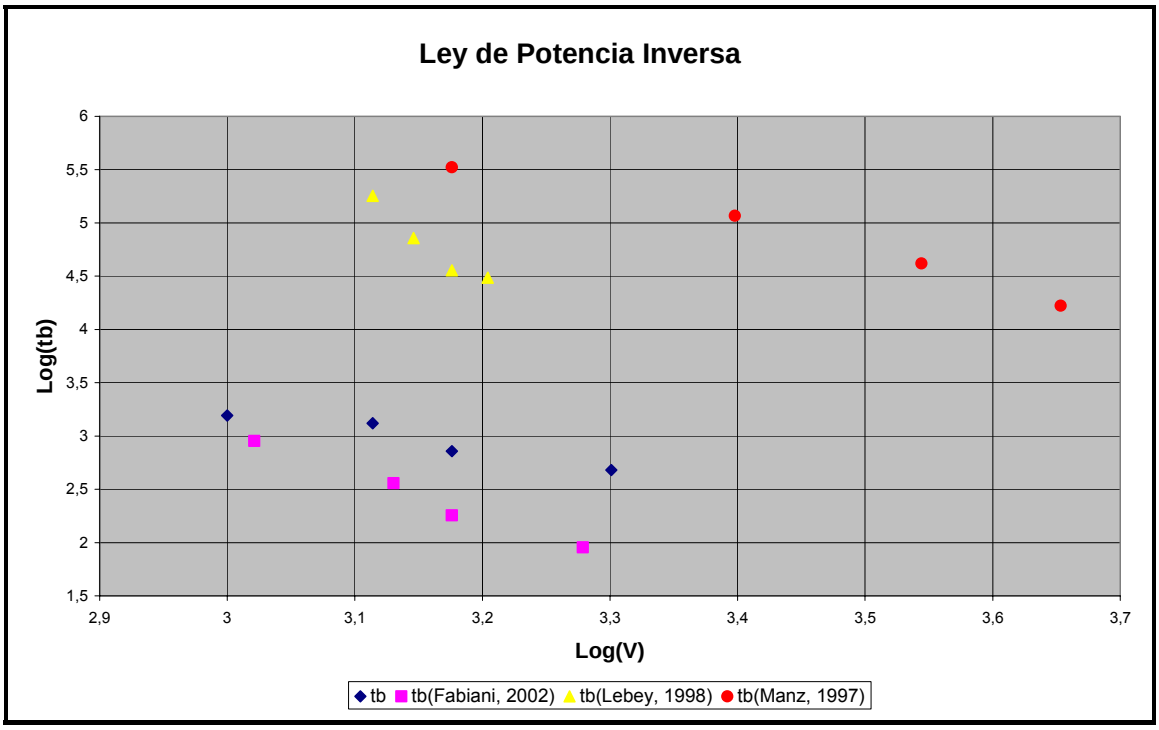

Figure 5.27.- Graphical representation for inverse power law accomplishment.

Nevertheless, extrapolation of this law to lower stress levels ([Manz, 1997]) and to other voltage waveforms are being currently discussed ([Guastavino, 2004]). [IEC 60505, 2004] remarks that the regression straight line may relate both magnitudes only in the limited voltage range chosen in order to have results in reasonable test times.

5.5.3.- Impregnated samples.

5.5.3.1.- PD detection analysis.

Despite PD activity spectra shape is similar to the expected one for this geometry ([CIGRE, 1969]), observation of conventional PD activity spectra, as has been shown in different works, does not give any indication about insulation status. That is the reason to deal with PD number versus rate and applied voltage phase 3D representation. From Figures 5.29g),h) and i) it can be concluded that there is a decrease in low charge magnitude PD rate, and an increase of PD number involving greater charge magnitudes compared to that of lower magnitudes.

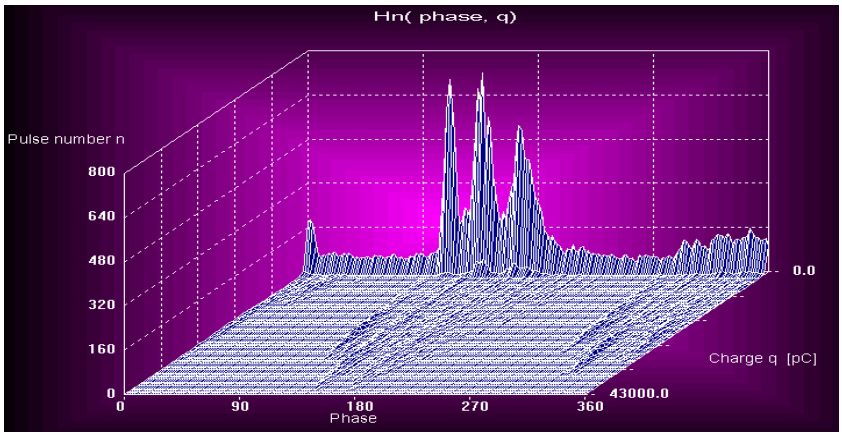

Figure 5.29g).- 3D representation of PD activity for sample MC4. Ageing time: 1min.

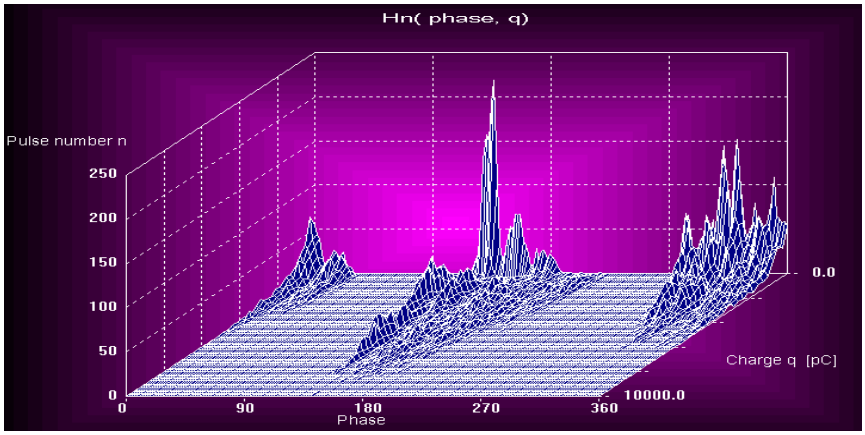

Figure 5.29h).- 3D representation of PD activity for sample MC4. Ageing time: 180min.

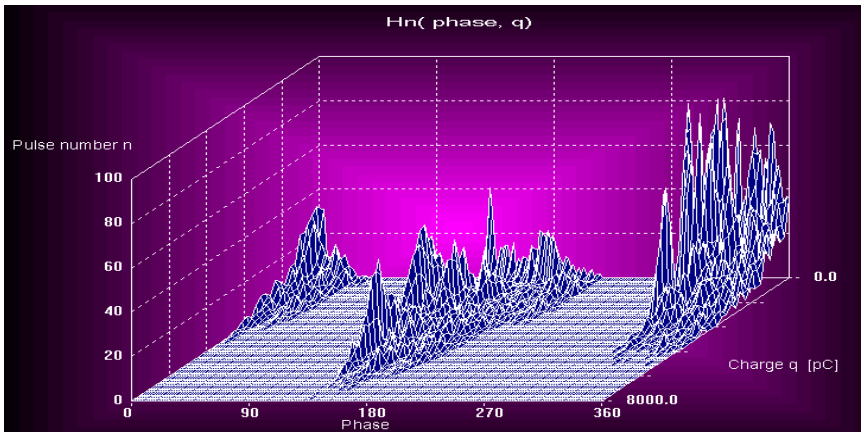

Figure 5.29i).- 3D representation of PD activity for sample MC4. Ageing time: 240min.

In order to summarize all these data, the Normalized Quantity Number NQN, has been proposed by [Lyles, 1988] as an integrated PD activity parameter given by the area under the curves PD rate-PD magnitude. Despite it is mentioned at [IEEE Std 1434, 2000], it is remarked that it is very difficult to extract any interpretation from these measurements. This can be confirmed by taking a look to our results presented in Table 5.5.

B4	NQN (t=10min)=58	NQN(t=180min)=-541	NQN(t=300min)=-2514
B2	NQN (t=10min)= -9325	NQN(t=60min)= -303	NQN(t=120min)= -1010
C4	NQN (t=1min)= -8679	NQN(t=180min)= -237	NQN(t=240min)= -123

Table 5.5.- NQN evolution for different dielectrics.

PD ageing patterns change from kind to kind of material, and even using the same material, PD spectra change too. It has not been localized any electrical parameter that may provide ageing degree determination due to PD activity ([Lin, 2004]). It has been made a great effort when using information contained in these PD spectra in order to detect insulating defects ([Krivda, 1995]) and the ageing degree without reaching to a definitive result ([Patsch, 2004]). This is our reason to work on other complementary diagnosis methods.

5.5.3.2.- Analysis by means of dielectric spectroscopy.

Tests made on twisted pair samples subjected to high PD activity, have shown a growing tendency in conductance $G=G(t,\omega)$ increases from its initial value ($G(t=0min,\omega)$) after some ageing time t in high frequency ranges ([Martínez, 2004]). In this section, this analysis has been applied to impregnated coils trying to set an indicator of PD ageing in insulation systems typically used in electrical motors. In order to get these data, turn-to-turn impedance ($Z=Z(\omega)$) in coils has been measured by means of FRA, so conductance can be obtained by:

$$G(\omega) = \mathrm{Re}\left[\frac{1}{Z(\omega)}\right] \qquad (5.3)$$

In Figures 5.30 it is shown the results obtained for those samples whose lifetime was wide enough to have as much experimental points about ageing as possible. Since it has been detected growing tendencies just for the curves $G=G(t)$ at certain frequencies $\omega=2*\pi*f$, it might be thought that there are certain conduction mechanisms activated at these frequencies. In these figures, it is shown the following parameter evolution with ageing time:

$$\Delta G = \frac{G_t(\omega,t) - G_0(\omega, t=0\,\mathrm{min})}{G_0(\omega, t=0\,\mathrm{min})} \qquad (5.4)$$

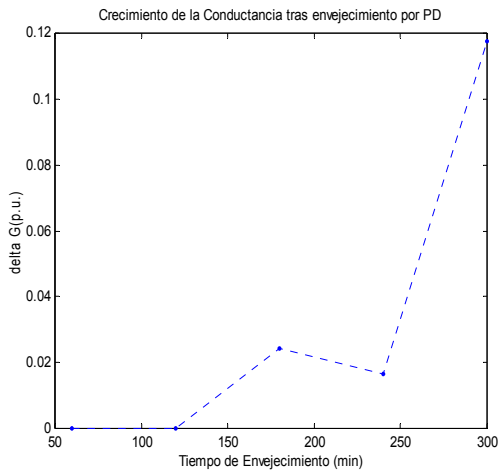

Figure 5.30a.- Sample MA6. f=2.3 MHz.

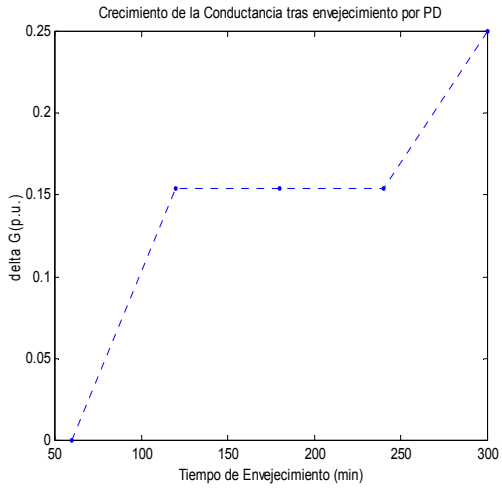

Figure 5.30b.- Sample MB4. f=3.9 MHz.

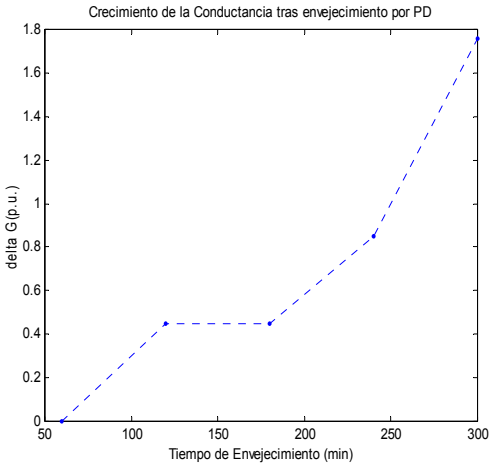

Figure 5.30c.- Sample MD2. f=6.5 MHz.

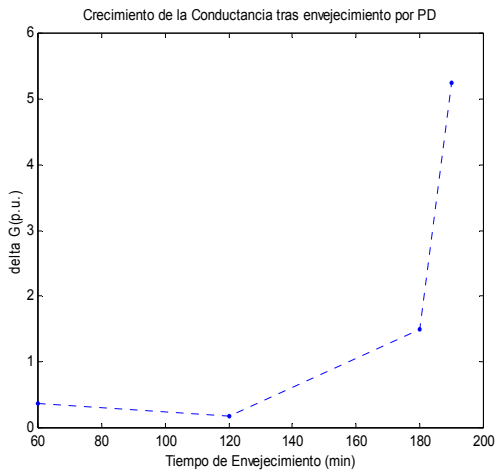

Figure 5.30d.- Sample MA1. f=21 MHz.

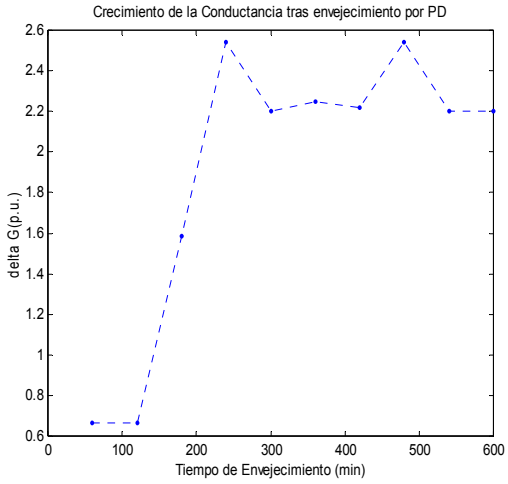

Figure 5.30e.- Sample MA2. f=15 MHz.

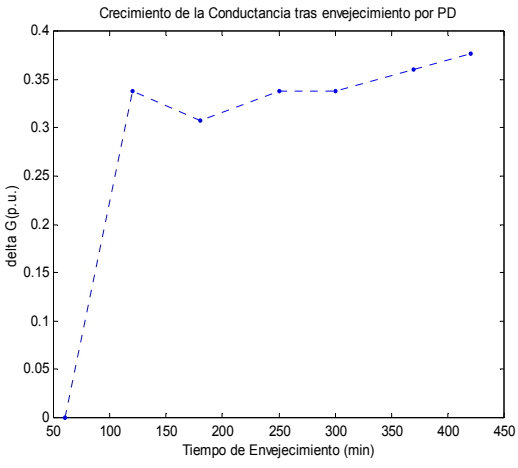

Figure 5.30f.- Sample MA3. f=30 MHz.

From the results presented here it is remarked that dielectric high frequency conductance grows with ageing time; this might be explained by the growth of imaginary part from complex electrical susceptibility ([Joncher, 1983]) due to power losses increase within the dielectric because of PD activity ([Bartnikas, 1979]).

The differences in frequencies selected to see conductance growths with ageing time are due to great differences between samples regarding to geometry and material. Since it was selected the widest spectrum to study any polarization phenomena, there were not so many experimental points in the frequency range were tendencies could be seen. Moreover, erratic behaviour in curve trends may be explained by practical differences in impregnating-curing processes that may provide changes in nature and geometry even with the same material.

The frequency range that allows studying insulation status suggests that the polarization mechanism that contains more information about dielectric ageing due to PD is dipolar polarization ([Von Hippel, 1966], [Zaengl, 2003]). This new indication about insulation status has not been pointed out at any previous work.

5.6.- Conclusions.

5.6.1.- Voltage distribution through impregnated coils.

In this chapter, it has been checked that the high frequency model for turn by turn voltage calculation through random wound coils is accurate for impregnated coils a well. Moreover, voltage calculation is reliable by using non-impregnated coil impedance measurements just taking into account changes in turn-to-turn and turn-to-ground capacitance values. These stray capacitances play a main role in voltage distribution through coils in inverter fed induction motor stators; in fact, it is possible to achieve a more even voltage propagation through coils by means of appropriate combinations in stray capacitances values.

5.6.2.- Turn to turn insulation status after accelerated ageing by PD.

Also, turn-to-turn insulation from different coils has been subjected to accelerated ageing cycles due to PD activity. Results from tests made on non-impregnated coils for different applied voltages, confirm inverse power law accomplishment. When dealing with impregnated samples, PD activity analysis does not provide useful information about insulation diagnosis. That is why turn-to-turn impedance FRA has been used looking for an insulation status indicator: high frequency conductance. Its growth with ageing time is due to high frequency dielectric susceptibility behaviour for different degradation degrees within the material. Dipolar polarization mechanism seems to be affected by PD activity in the dielectric material.

6.- Conclusions and future work.

6.1.- Conclusions.

In this Thesis, it has been introduced the problem produced at low voltage induction motors when fed by electronic converters. State of the art review and present results remark that these steep fronted pulses are responsible for insulation systems' mean lifetime reduction and, indeed, machines' one.

These voltage transients are so aggressive to insulation systems because, as presented in previous works, in machines with form wound coils turn by turn voltage distribution is uneven. Moreover, in random wound coils (as those used in low voltage motors), it has been shown that during transient times nearly the whole voltage falls in the machine's firsts coils, so just enamel thickness have to withstand voltages out of its rated conditions, as specified by the manufacturer. These new electrical stresses enhance different ageing mechanisms at each insulation system through the motor, but, whatever, they always lead to high PD activity.

These were the reasons to face this work, whose main conclusions are reviewed now:

1) It was developed a distributed parameter model for turn by turn voltage calculation through random wound coils, firstly with a low number of turns. In this model, equations were set in the frequency domain, so it can be can be taken into account certain equivalent circuit parameters dependence with frequency. In order to apply this model it is necessary to characterize each unit cell's impedance (single turn impedance, turn-to-turn and turn-to-ground impedance) within the proper bandwidth, and set necessary approximations to certain high frequency electromagnetic phenomena (proximity effect and mutual inductances) that take place in the coil but were neglected in other works. This model allowed to calculate accurately high frequency voltage distribution through a five-turns random wound coil, by means of a reduced set of impedance measurements.
2) Model reliability was proven at different five-turns coils as well so it was checked that the random nature of the coils does not affect model prediction capability.
3) Deep analysis of voltage transients propagation through coils in a real induction motor showed that also in random wound coils voltages through turns are distributed in an uneven way, so during certain periods of time, the whole applied voltage will be displayed between firsts and lasts turns in the coil.
4) Through the results from the same experimental setup (on this purpose we counted on the help the Electrical Engineering Department at University Paul Sabatier-CNRS at Toulouse), it was checked how the lack of uniformity in turn by turn voltage distribution (that provides greater turn to turn voltages) is greater as applied voltage rise times are lower.
5) Results from point 3) are very useful in order to apply model proposal from point 1) to a coil with higher number of turns because it allowed to have a more realistic

knowledge of the problem to face and to simplify the model in order to reach the most important objective: set a model for voltage prediction through the turns along the coil subjected to higher electrical stresses. So these previous results allowed to properly approach to the application of this calculation model to a random wound coil with higher number of turns inserted in a real low voltage machine stator. In the same way as before, calculation was accurately made by means of a reduced number of impedance measurements and by using a distributed parameter model whose equations were described in the frequency domain.

6) Dielectric losses from turn-to-turn and turn-to-ground impedances have no influence in model accuracy. This conclusion is common from model application at points 1) and 5).
7) Losses from skin and proximity effect cannot be neglected in the model, because on the contrary, calculation errors arise. Voltage phase calculation was more affected by this effect at a 5 turns coil (point 1)) and a 49 turns coil (point 5)) as well. This result is not in accordance with those presented at other works with higher rise times ([Narang, 1989]). It should be remarked that in the wide frequency ranges under study nowadays, it is mandatory to distinguish between these losses and those arisen from dielectrics despite it had not be done in this way previously ([Wright, 1983]); nevertheless there are recent works that point to this direction ([Oyegoke, 2000]).
8) Neglecting mutual inductances has a bad influence in turn by turn high frequency voltage calculation. Its influence was greater for voltage magnitudes for both kinds of coils (5 or 49 turns as well).
9) The model from previous sections made high frequency transfer functions calculation for all winding turns indeed; they allow to calculate winding response to voltage pulses in the time domain by means of fast Fourier transform. Frequency domain model reliability gives accurate calculations in the time domain, and this is completely confirmed by direct measurements through turns into a winding fed by voltage pulses with the same amplitude and rise time than those used in Fourier transformation. As it was exposed in chapter 2, a prediction model for turn by turn voltage calculation through random wound coils subjected to steep fronted pulses was a problem to be solved and it has been faced successfully in this thesis.
10) Applying this technique from previous section allows calculating winding response to transient overvoltages similar to those found in real industrial environments. Analysis from these results reveals that it is pretty possible that two wires subjected to voltages magnitudes similar to input maximum ones may be in physical contact.
11) The model is accurate when calculating turn by turn voltages through coils impregnated with different resins as well. From the bibliography, it has not been found any methodology checking calculation capability for different dielectrics, challenge successfully faced in this work.
12) The model can be used to calculate voltages through impregnated coils by means of stray capacitance measurements (resulting from varnishing processes) and remaining impedances from non-impregnated samples. Stray capacitances have a strong influence in high frequency voltage propagation through coils; model application confirms this statement presented in many previous works.
13) Model application, modifying equivalent circuit parameters in an appropriate way, leads to a lower magnitude turn-to-turn electrical stresses distribution. The need of increasing *Ctt/Ctg* ratio in order to achieve a turn by turn voltage distribution as

much uniform as possible, has not been mentioned recently, and the only justification found to this is based upon analytical approaches to winding models without experimental confirmation ([Wagner, 1915], [Dormont, 1971]).

14) Regarding to PD accelerated ageing studies in turn-to-turn insulation systems, despite inverse power law has been confirmed, it has been shown difficulties in diagnosis from PD activity patterns data. This was the reason to present high frequency conductance as a new indicator about insulation system status during PD ageing. Despite there are some published works about frequency domain spectroscopy, this parameter has not been ever mentioned in the read bibliography, so this might be considered as a new approach to machine's insulation off-line diagnosis.
15) The frequency ranges where dielectric diagnosis was made by means of conductance, point to dipolar polarization as the mechanism that shows more information about PD ageing process in epoxi resins.

6.2.- Original contributions.

1) In this thesis it is presented the first model (at least to the author's knowledge) to calculate turn by turn voltage distribution for random wound coils fed by steep fronted pulses whose rise time is in the tens of nanoseconds range.
2) When analysing these transients, losses due to skin and proximity effects and mutual inductances must be included in the prediction model. Proximity effect modelling is brand new and it should be remarked that its frequency dependence must be taken into account in order to make accurate calculations.
3) In each phase from an induction motor subjected to steep fronted transients, greatest electrical stresses take place in first coils, so nearly the whole applied phase voltage will subject two enamelled wires to stresses that exceed the manufacturing conditions.
4) This is the first work where it has been quantified the *Ctt/Ctg* ratio variation to reach a more uniform voltage distribution through the winding.
5) In this thesis, it has been presented high frequency conductance as a promising new status indicator for turn-to-turn insulation when subjected to PD ageing processes.

6.3.- Future work.

1) Study the effect of these transients on coils from different phases placed in the same slots.
2) Study the possibility of extracting each distributed parameter impedance from motor external measurements. This would allow to have the calculation model ready without using a stator prototype as used at chapter 4.
3) Model application to winding designs more resistant to steep fronted transients. Firstly, the knowledge about the points in the first coil where there are greater electrical stresses on the basis of a reduced number of measurements, allows preventing from premature failures by using insulation reinforcements in certain

winding areas. Afterwards, it could be studied the possibility of achieving *Ctt* and *Ctg* values that would lead to a more uniform voltage distribution through coils in low voltage motor stators.

4) Make deeper studies on breakdown mechanisms that lead to premature failure in machines subjected to steep fronted voltage pulses. Up to now, it is not clear if there is dielectric ageing in absence of PD. It is interesting to make more studies about the effect that new voltage waveshapes may have on materials designed to work for lower *du/dt* values.
5) Development of on-line PD detection systems in inverter fed drives. This would be helpful in machine diagnosis but, up to the date, its technical problems remain unsolved.
6) FRA technique should be extended to status diagnosis in insulation systems subjected to PD's. Despite results presented here about high frequency conductance seems to open a new research trend to follow, this phenomenon must be analysed on more samples and other materials. However, it should be done a deeper approach to the physics behind the problem to check if dipolar polarization is the mechanism that shows material PD ageing signs.

Bibliography:

[Al-Ghubari, 2001] Al-Ghubari F.H., Von Jouanne A., Wallace A.K., "The Effects of PWM Inverters on the Winding Voltage Distribution in Induction Motors", Electric Power Components and Systems, 2001.

[Al-Zamil, 2003] Al-Zamil A.M., Saied M.M., Al-Jalahmah T.N., "Suppression of over-voltage switching transients of PWM motor drives using passive filtering technique", XIIIth International Symposium on High Voltage Engineering, 2003.

[Aoki, 1999] Aoki N., Satoh K., Nabae A., "Damping Circuit to Suppress Motor Terminal Overvoltage and Ringing in PWM Inverter-Fed AC Motor Drive Systems with Long Motor Leads", IEEE Transactions on Industry Applications, 1999.

[Bartinkas, 1979] Bartnikas, McMahon, "Engineering Dielectrics: Volume I, Corona Measurement and Interpretation", ASTM, 1979.

[Bellomo, 1996] Bellomo J.P., Lebey T., Oraison J.M., Peltier F., "Influence of Rise Time on the Dielectric Behavior of Stator Insulation Materials", Conference on Electrical Insulation and Dielectric Phenomena, 1996.

[Bellomo, 1998] Bellomo J.P., Dinculescu S., Lebey T., "Lifetime of Conventional and Corona Resistant Enamels", IEEE International Symposium on Electrical Insulation, 1998.

[Bellomo, 1999] Bellomo J.P., Castelan P., Lebey T., "The Effect of Pulsed Voltages on Dielectric Material Properties", IEEE Transactions on Dielectrics and Electrical Insulation, 1999.
[Bidan, 2001] Bidan P., Lebey T., Montseny G., Neacsu C., Saint-Michel J., "Transient Voltage Distribution in Inverter Fed Motor Windings: Experimental Study and Modeling", IEEE Transactions on Power Electronics, 2001.

[Bidan, 2003] Bidan P., Lebey T., Neacsu C., "Development of a New Off-Line Test Procedure for Low Voltage Rotating Machines Fed by Adjustable Speed Drives (ASD)", IEEE Transactions on Dielectrics and Electrical Insulation, 2003.

[Böhm, 2002] Böhm F., Schindler H., Nagel K., "Voltron^{TM} – A New Generation of Wire Enamel for the Production of Magnet Wires for Inverter Fed Motors", INSUCON 2002, 2002.

[Bonnett, 1998] Bonnett A.H., "Available Insulation Systems for PWM Inverter-Fed Motors", IEEE Industry Applications Magazine, 1998.
[Bravo de Medina, 1998] Bravo de Medina N., "Sobreoscilaciones. Teoría", Automática e Instrumentación, 1998.
[Briz, 2004] Briz F., Degner M.W., Diez A.B., Guerrero J.M., "Online Diagnostics in Inverter-Fed Induction Machines Using High-Frequency Signal Injection", IEEE Transactions on Industry Applications, 2004.
[Busch, 2002] Busch R., Pohlmann F. Mueller K., "Insulating Systems for Three-Phase Current Low-Voltage Motors Controlled By PWM Inverters: State of Development and Applications Aspects", INSUCON 2002, 2002.

[Cabanelas, 2001] Cabanelas JC, Serrano B, González-Benito J, Bravo J, Baselga J., "Macromolecular Rapid Communications", 22, 694, 2001.

[Campbell, 1994] Campbell S.R., Stone G.C., Sedding H.G., Klempner G.S., McDermid W., Bussey R.G., "Practical On-Line Partial Discharge Tests for Turbine Generators and Motors", IEEE Transactions on Energy Conversion, 1994.
[Casal, 2000] Casal M., Burgos M., Izquierdo C., "Sistema de Aislamiento en Motores Eléctricos de Alta Tensión. Envejecimiento, Ensayos y Diagnosis", Energía, 2000.
[Churchill, 1987] Churchill T.L., Edmonds J.S., "Rotor-Mounted Scanning of Distressed Armatures in Hydrogeneratos", Electrical and Electronics Insulation Conference, 1987.
[CIGRE, 1969] CIGRE, "Recognition of Discharges", Electra, 1969.
[CIGRE, 1998] G.C. Stone, S.R. Campbell, H.G. Sedding, "Analysis of the Effect of Adjustable Speed Drive Surges on Motor Stator Winding Insulation", CIGRE Session, 1998.
[Contin, 1993] Contin A., Rabach G. "PD Analysis of Rotating AC Machines", IEEE Transactions on Electrical Insulation, 1993.
[Contin, 2003] Contin M.C., Bastos J.P.A., Sadowski N., "Failures in Motors fed by Static Converters: Causes and Solutions", 8º Congresso Luso Espanhol de Engenharia Electrotécnica, 2003.

[Devins, 1984] Devins, J C, "The Physics of Partial Discharges in Solid Dielectrics", IEEE Transactions on Electrical Insulation, 1984.
[Dormont, 1971] Dormont M.J., "Cálculo y construcción de las máquinas eléctricas estáticas: Transformadores", 1971.

[Fabiani, 2001] Fabiani D., Montanari G.C., Contin A., "Aging Acceleration of Insulating Materials for Electrical Machine Windings Supplied by PWM in the Presence and the Absence of Partial Discharges", IEEE International Conference on Solid Dielectrics , 2001.
[Fenger, 2003] Fenger M., Campbell S.R., Pedersen J., "Motor Winding Problems Caused by Inverter Drives", IEEE Industry Applications Magazine, 2003.

[Fernández, 2001] Fernández Cabanas M., "Diagnóstico Precoz de Fallos en el Sistema Aislante de los Motores Asíncronos de Media Tensión: Ventajas y Limitaciones de los Ensayos Clásicos y los Nuevos Métodos Experimentales", VII Jornadas Hispano-Lusas de Ingeniería Eléctrica, 2001.
[Florkowski, 2003] Florkowski M., Furgal J., Saaranen J., "Motor winding quality assessment based on frequency response analysis", XIIIth International Symposium on High Voltage Engineering, 2003.
[Fothergill, 2004] Fothergill J., "Electrical Ageing of Dielectrics", IEEE International Conference on Solid Dielectrics, 2004.

[Gäfvert, 2000] Gäfvert U., Adeen L., Tapper M., Ghasemi P., Jönsson B., "Dielectric Spectroscopy in Time and Frequency Domain Applied to Diagnostics of Power Transformers", International Conference on Properties and Applications of Dielectric Materials, 2000.
[Greenwood, 1991] Greenwood A, "Electrical Transients in Power Systems", John Wiley and Sons, 1991.
[Guardado, 1989] Guardado J.L., Cornick K.J., "A Computer Model for Calculating Steep-Fronted Surge Distribution in Machine Windings", IEEE Transactions on Energy Conversion, 1989.

[Guardado, 1992] Guardado J.L., Cornick K.J., "The Effect of Coil Parameters on the Distribution of Steep-Fronted Surges in Machine Windings", IEEE Transactions on Energy Conversion, 1992.
[Guardado, 1996] Guardado J.L., Cornick K.J., "Calculation of Machine Winding Electrical Parameters at High Frequencies for Switching Transient Studies", IEEE Transactions on Energy Conversion, 1996.

[Guastavino, 2004] Guastavino F., Coletti G., Dardano A, Torello E., "Life tests on twisted pairs subjected to PWM-like voltages", IEEE International Conference on Solid Dielectrics, 2004.

[Gubbala, 1995] Gubbala L., Von Jouanne A., Enjeti P., Singh C., Toliyat H., "Voltage Distribution in the Windings of an AC Motor Subjected to High dv/dt PWM Voltages", Power Electronics Specialists Conference, 1995.

[Guilhaume-Chaillot, 2004] Guilhaume-Chaillot A., Munier C., Richet S., Arnoud F., "New dielectric materials: How to control their reliability in avionics environment for a long term period?", IEEE International Conference on Solid Dielectrics, 2004.

[Hanigovszki, 2004] Hanigovszki N., Poulsen J., Blaabjerg F., "A Novel Output Filter Topology to Reduce Motor Overvoltage", IEEE Transactions on Industry Applications, 2004.

[Humiston, 2004] Humiston T., Pillay P., "Experimental Setup for the Measurement of Surge Propagation in Induction Machines", IEEE Transactions on Energy Conversion, 2004.

[Hwang, 2003] Hwang D.-H., Lee K.-C., Kim Y.-J., Bae S.-W., Kim D.-H., Ro C.-G., "Voltage Stresses on Stator Windings of Induction Motors Driven by IGBT PWM Inverters", Industry Applications Conference, 2003.

[IEC 60505, 2004] IEC 60505, "Evaluation and qualification of Electrical Insulation Systems", IEC Standard, 2004.

[IEC 60034-25, 2004] IEC 60034-25, "Guide for the design and performance of cage induction motors specifically designed for converter supply", IEC Technical Specification, 2004.

[IEC 60034-17, 2004] IEC 60034-17, "Cage Induction Motors When Fed From Converters", IEC Application Guide, 2004.

[IEEE Std 522, 1992] IEEE Std 522-1992, "IEEE Guide for Testing Turn-to-Turn Insulation on Form-Wound Stator Coils for Alternating-Current Rotating Electric Machines", 1992.

[IEEE Std 1434, 2000] IEEE Std 1434-2000, "IEEE Trial-Use Guide to the Measurement of Partial Discharges in Rotating Machinery", 2000.

[Islam, 1997] Islam S., Ledwich G., "An Equivalent Circuit for Calculation of Interturn Voltage Distribution of Stator Windings in the Presence of Slot Discharges", IEEE International Conference on properties and applications of dielectric materials, 1997.

[Jianru, 2001] Jianru W., Zhiqiang L., Huanjun Y., "Research of PWM Pulse Voltage Distribution in Motor Winding", Proceedings of 5th International Conference on Electrical Machines and Systems, 2001.

[Jianru, 2002] Jianru W., Hongchi L., Huanjun Y., "Voltage Distribution in Stator Windings of the Motor Driven by PWM Inverter", Proceedings of Power System Technology Conference, 2002.

[Jonscher, 1983] Jonscher, "The Universal Dielectric Response", IEEE Electrical Insualtion Magazine, 1983.

[Karsai, 1987] Karsai K., Kerényi D., Kiss L., "Large Power Transformers", 1987.

[Kaufhold, 1996] Kaufhold M., Börner G., Eberhardt M., Speck J., "Failure Mechanism of the Interturn Insulation of Low Voltage Electric Machines Fed by Pulse-Controlled Inverters", IEEE Electrical Insulation Magazine, 1996.

[Kerkman, 1997] Kerkman R.J., Leggate D., Skibinski G.L., "Interaction of Drive Modulation and Cable Parameters on AC Motor Transients", IEEE Transactions on Industry Applications, 1997.

[Khalifa, 1990] Khalifa M., "High Voltage Engineering. Theory and Practice", Marcel Dekker, 1990.

[Krivda, 1995] Krivda A., "Recognition of Discharges. Discrimination and Classification", Delft, 1995.

[Kueck, 2002] Kueck J.D., Haynes H. D., Staunton R.H., "Stator Insulation Degradation Test Uses ASD Switching Frequency", IEEE Power Engineering Review, 2002.
[Lanier, 1999] Lanier C., "Using Corona Inception Voltage for Motor Evaluation", IEEE Industry Applications Magazine, 1999.
[Lathi, 1992] Lathi B.P., "Modern Digital and Analog Communication Systems", 1989.
[Lebey, 1998] Lebey T., Castelan P., Montanari G.C., Ghinello I., "Influence of PWM-Type Voltage Waveforms on Reliability of Machine Insulation System", International Conference on Harmonics and Quality of Power, 1998.

[Lee, 2002] Lee S., Nam K., "An Overvoltage Suppression Scheme for AC Motor Drives Using Half DC-Link Voltage level at Each PWM Transition", IEEE Transactions on Industrial Electronics, 2002.
[Lee, 2004] Lee S., Nam K., "Overvoltage Suppression Filter Design Methods Based on Voltage Reflection Theory", IEEE Transactions on Power Electronics, 2004.

[Lemke, 1999] Lemke Diagnostics GmbH, "Partial Discharge Diagnostics: LDS-6 User's Manual", Measuring Equipment Training Courses,1999.

[Liu, 2004] Liu J., Pillay P., Douglas H., "Wavelet Modeling of Motor Drives Applied to the Calculation of Motor Terminal Overvoltages", IEEE Transactions on Industrial Electronics, 2004.

[Lin, 2004] Lin T., Zhang G., Zhan L., Zhang L., "Study on Ageing Properties of Magnet Wires' Insulation Used for Electric Locomotive Pulling Motors", IEEE International Conference on Solid Dielectrics, 2004.

[Lyles, 1988] Lyles J.F., Stone G.C., Kurtz M., "Experience with PDA Diagnostic Testing on Hydraulic Generators", IEEE Transactions on Energy Conversion, 1988.
[Lupo, 2002] Lupo G., Petrarca C., Vitelli M., Tucci V., "Multiconductor Transmisión Line Análysis of Steep-front Surges in Machine Windings", IEEE Transactions on Dielectrics and Electrical Insulation, 2002.

[MacDonald, 1999] MacDonald D., Gray W., "PWM Drive Related Bearing Failures", IEEE Industry Applications Magazine, 1999.
[Manz, 1997] Manz L., "Motor Insulation System Quality for IGBT Drives", IEEE Industry Applications Magazine, 1997.
[Martínez, 2004] J.M. Martínez Tarifa, J.Sanz Feito, H. Amarís Duarte; "Turn to Turn Insulation Ageing Diagnosis Using Frequency Response Analysis"; IEEE International Conference on Solid Dielectrics; Toulouse (Francia); 2004.
[Martínez, 2005] J.M Martínez Tarifa, H. Amarís Duarte, J. Sanz Feito; "Frequency domain modeling of random wound motor winding for insulation stress analysis"; Electrical Engineering; Springer; 2005.
[May, 1988] May, C.A, "Epoxi resins", Chemistry and Technology, 1988.
[Mbaye, 1997] Mbaye A., Bellomo J.P., Lebey T., Oraison J.M., Peltier F., "Electrical Stresses Applied to Stator Insulation in Low-Voltage Induction Motors Fed by PWM Drives", IEE Proceedings of Electric Power Applications, 1997.
[Mbaye, 1998] Mbaye A., Lebey T, "Analytical Approach of PD Activity in Low Voltage Motors Fed by Inverters", IEEE International Conference on Conduction and Breakdown in Solid Dielectrics, 1998.

[McDermid, 1993] McDermid W., "Insulation Systems and Monitoring for Stator Windings of Large Rotating Machines", IEEE Electrical Insulation Magazine, 1993.
[McLaren, 1988] McLaren P.G., Abdel-Rahman M.H., "Modelling of Large AC Motor Coils for Steep-Fronted Surge Studies", IEEE Transactions on Industry Applications, 1988.
[Melfi, 1998] Melfi M., Sung A.M.J., Bell S., Skibinski G., "Effect of Surge Voltage Risetime on the Insulation of Low-Voltage Machines Fed by PWM Converters", IEEE Transactions on Industry Applications, 1998.

[Mukundan, 2004] Mukundan T.R., "Calculation of Voltage Surges on Motors Fed From PWM Drives- A Simplified Approach", IEEE Transactions on Energy Conversion, 2004.

[Narang, 1989] Narang A., Gupta B.K., Dick E.P., Sharma D.K., "Measurement and Analysis of Surge Distribution in Motor Stator Windings", IEEE Transactions on Energy Conversion, 1989.
[Neacsu, 2002] Neacsu C., "Contribution à L'Etude des Défaillances Statoriques des Machines Asynchrones : Mise au Point et Réalisation d'un Test Non Destructif de Fin de Fabrication", These du grade de Docteur de L'Universite Paul Sabatier, 2002.

[Oppenheim, 1997] Oppenheim A.V., Willsky A.S., "Signals and Systems", 1997.

[Oyegoke, 2000] Oyegoke B.S., "Voltage Distribution in the Stator Winding of an Induction Motor Following a Voltage Surge", Electrical Engineering, 2000.
[Oyegoke, 2001] Oyegoke B., Hyvönen P., Aro M., "Dielectric Response Measurement as Diagnostic Tool for Power Cable Systems", Helsinki University of Technology Report, 2001.
[Oyegoke, 2000] Oyegoke B.S., "A comparative analysis of methods for calculating the transient voltage distribution within the stator winding of an electric machine subjected to steep-fronted surge", Electrical Engineering, 2000.

[Pascault, 2002] Pascault J.P., Sautereau H., Verdu J., Williams R.J.J., "Thermosetting Polymers", Ed. Marcel Dekker Inc., 2002.
[Patsch R., 2002] Patsch R., Berton F., "Pulse Sequence Analysis -a diagnostic tool based on the physics behind partial discharges", Journal of Physics D: Applied Physics, 2002.

[Patsch R., 2004] Patsch R., Benzerouk D., "Characterization of Partial Discharge Processes –what Parameters work best?", IEEE International Conference on Solid Dielectrics, 2004.

[Petrarca, 2000] Petrarca C., Lupo G., Tucci V., Vitelli M., "The Influence of Coil Parameters on the Voltage Distribution in a Machine Stator Winding Fed by a PWM Inverter", 2000 Conference on Electrical Insulation and Dielectric Phenomena, 2000.

[Petrarca, 2004] Petrarca C., Maffucci A., Tucci V., Vitelli M., "Analysis of the Voltage Distribution in a Motor Stator Winding Subjected to Steep-Fronted Surge Voltages by Means of a Multiconductor Lossy Transmission Line Model", IEEE Transactions on Energy Conversion, 2004.

[Pfeiffer, 1999] Pfeiffer W., Paede M., "About the Influence of Frequency on the Partial Discharge Characteristics of Enamelled Wires", Electrical Insulation Conference, 1999.
[Pleite, 2001] Pleite J., Olías E., Barrado A., Lázaro A., Vázquez J., "Herramienta de Modelado para Análisis F.R.A. de Transformadores", 7ª Jornadas Hispano-Lusas de Ingeniería Eléctrica, 2001.

[Popov, 2003] Popov M., Van der Sluis L., Paap G.C., De Herdt H., "Computation of Very Fast Transient Overvoltages in Transformer Windings", IEEE Transactions on Power Delivery, 2003.

[Popovic, 1970] Popovic B.D., "Introductory Engineering Electromagnetics", Addison-Wesley, 1970.

[Pouilles, 1995] Pouilles V., Lebey T., Chênerie I., Bui A., "Correlation between Energy Dissipation and Permitivity in Dielectric Material Ageing Studies", International Symposium on High Voltage Engineering, 1995.

[Shackleford, 1998] Shackleford J.F., "Introducción a la Ciencia de Materiales para Ingenieros", Prentice Hall, 1998.

[Solartron, 2001] Solartron Analytical, "Solartron 1260 Impedance/Gain-Phase Analyser Operating Manual", 2001.

[Stone, 1988] Stone G.C., Sedding H.G., Lloyd B.A., Gupta B K, "The Ability of Diagnostics Tests to Estimate The Remaining Life of Stator Insulation", IEEE Transactions on Energy Conversion, 1988.

[Stone, 2000] Stone G., Campbell S., Tetreault S., "Inverter-Fed Drives: Which Motor Stators are at Risk?", IEEE Industry Applications Magazine, 2000.

[Stone, 2001] Stone G.C., Campbell S.R., Discussion of "Field Experiences on the Measurement of Partial Discharges on Rotating Equipment", IEEE Transactions on Energy Conversion, 2001.

[Stone, 2005] Stone G.C., "Recent Important Changes in IEEE Motor and Generator Winding Insulation Diagnostic Testing Standards", IEEE Transactions on Industry Applications, 2005.

[Stranges, 2003] Stranges N., Dymond J.H., "How Design Influences the Temperature Rise of Motors on Inverter Drives", IEEE Transactions on Industry Applications, 2003.

[Suresh, 1997] Suresh G., Toliyat H.A., Rendussara D.A., Enjeti P.N., "Predicting the Transient Effects of PWM Voltage Waveform on the Stator Windings of Random Wound Induction Motors", American Power Electronics Conference, 1997.

[Tang, 1997] Tang Y., "Analysis of Steep-Fronted Voltage Distribution and Turn Insulation Failure in Inverter Fed AC Motor", IEEE Industry Applications Conference, 1997.

[Toliyat, 1999] Toliyat H.A., Suresh G., Abur A., "Estimation of Voltage Distribution on the Inverter Fed Random Wound Induction Motor Windings Supplied through Feeder Cable", IEEE Transactions on Energy Conversion, 1999.

[UNE-EN 60851-5, 1997] UNE-EN 60851-5, "Hilos para Bobinas Electromagnéticas. Métodos de Ensayo. Parte 5: Propiedades Eléctricas", 1997.

[Von Jouanne, 1996] Von Jouanne A., Rendusara D.A., Enjeti P.N., Gray J.W., "Filtering Techniques to Minimize the Effect of Long Motor Leads on PWM Inverter-Fed AC Motor Drive Systems", IEEE Transactions on Industry Applications, 1996.

[Von Hippel, 1966] Von Hippel A.R. et al, "Dielectric Materials and Applications", Massachusetts Institute of Technology Press, 1966.

[Wagner, 1915] Wagner K.W., "Das Eindringen einer Elektromagnetischen Welle in eine Spule mit Windungskapazität", Elektrotechnik und Maschinenbau, 1915.

[Wait, 1992] Wait J.V., Huelsman L.P., Korn G.A., "Introducción al amplificador operacional. Teoría y aplicaciones", Gustavo Gili, 1992.
[Wen, 2004] Wen F., Zhang L., Wu G., He E., "Modeling and Simulation of Inter-turn Voltage Distribution in the Stator Windings of Pulling Motor", IEEE International Conference on Solid Dielectrics, 2004.
[Wendel, 2002] Wendel C., Drpic M., Hoof M., "Insulation Systems in Inverter Fed Machines. A New Test Arrangement for Qualification", INSUCON 2002, 2002.

[Wright, 1983] Wright M.T., Yang S.J., McLeay K, "General Theory of Fast Fronted Interturn Voltage Distribution in Electrical Machine Windings", IEE Proceedings, 1983.
[Yazici, 2004] Yazici B., "Statistical Pattern Analysis of Partial Discharge Measurements for Quality Assessment of Insulation Systems in High-Voltage Electrical Machinery", IEEE Transactions on Industry Applications, 2004.
[Yin, 1997] Yin W., Bultemeier K., Barta D., Floryan D., "Improved Magnet Wire for Inverter-Fed Motors", Proceedings of Electrical Insulation Conference and Electrical Machinery, 1997.
[Yin, 1997] Yin W., "Failure Mechanism of Winding Insulations in Inverter-Fed Motors", IEEE Electrical Insulation Magazine, 1997.
[Yung, 2004] Yung C., Bonnett A.H., "Repair or Replace?. A decision model for industrial electric motors", IEEE Industry Applications Magazine, 2004.

[Zaengl, 2003] W.S. Zaengl, "Dielectric Spectroscopy in Time and Frequency Domain for HV Power Equipment, Part I: Theoretical Considerations", Dielectrics and Electrical Insulation Magazine, 2003.